Citation for published version:
Nathubhai, A, Haikarainen, T, Hayward, PC, Munoz-Descalzo, S, Thompson, AS, Lloyd, MD, Lehtio, L & Threadgill, M 2016, 'Structure-activity relationships of 2-arylquinazolin-4-ones as highly selective and potent inhibitors of the tankyrases', *European Journal of Medicinal Chemistry*, vol. 118, pp. 316-327. https://doi.org/10.1016/j.ejmech.2016.04.041

DOI:
10.1016/j.ejmech.2016.04.041

Publication date:
2016

Document Version
Peer reviewed version

Link to publication

Publisher Rights
CC BY-NC-ND

University of Bath

Alternative formats
If you require this document in an alternative format, please contact:
openaccess@bath.ac.uk

General rights
Copyright and moral rights for the publications made accessible in the public portal are retained by the authors and/or other copyright owners and it is a condition of accessing publications that users recognise and abide by the legal requirements associated with these rights.

Take down policy
If you believe that this document breaches copyright please contact us providing details, and we will remove access to the work immediately and investigate your claim.

Download date: 06. May. 2023

Structure-activity relationships of 2-arylquinazolin-4-ones as highly selective and potent inhibitors of the tankyrases

Amit Nathubhai,[a,*] Pauline J. Wood,[a] Teemu Haikarainen,[b] Penelope C. Hayward,[c] Silvia Muñoz-Descalzo,[d] Andrew S. Thompson,[a] Matthew D. Lloyd,[a] Lari Lehtiö[b] and Michael D. Threadgill[a]

[a] Medicinal Chemistry, Department of Pharmacy and Pharmacology, University of Bath, Claverton Down, Bath BA2 7AY, UK

[b] Biocenter Oulu and Faculty of Biochemistry and Molecular Medicine, University of Oulu, Oulu, Finland

[c] Department of Genetics, University of Cambridge, Downing Street, Cambridge CB2 3EH, UK

[d] Department of Biology and Biochemistry, University of Bath, Claverton Down, Bath BA2 7AY, UK

Keywords[†]

Tankyrase, PARP, 2-arylquinazolin-4-one, Wnt, hydrophobic cavity

Highlights

- Structure-Activity Relationship of 2-arylquinazolin-4-ones as tankyrase inhibitors
- 8-Methyl group gives selectivity for tankyrases over PARP-1 and PARP-2
- Polar groups at the 8-position give poor isoform-selectivity
- Crystal structures rationalised the observed selectivity
- Reveal a novel, potent and selective tankyrase and Wnt signalling inhibitor

Abstract

Tankyrases (TNKSs), members of the PARP (Poly(ADP-ribose)polymerases) superfamily of enzymes, have gained interest as therapeutic drug targets, especially as they are involved in the regulation of Wnt signalling. A series of 2-arylquinazolin-4-ones with varying substituents at the 8-position was synthesised. An 8-methyl group (compared to 8-H, 8-OMe, 8-OH), together with a 4'-hydrophobic or electron-withdrawing group, provided the most potency and

[*] Corresponding author: Telephone +44 1225 383379; FAX +44 1225 386114; e-mail a.nathubhai@bath.ac.uk

[†] Abbreviations: ADP, adenosine diphosphate; Bn, benzyl; Cbz, benzyloxycarbonyl; DMAP, 4-dimethylamino-pyridine; EDC, N'-ethyl-N-3-(dimethylaminopropyl)carbodiimide; ES, electrospray; HMBC, heteronuclear multiple-bond correlation spectroscopy; HSQC, heteronuclear single quantum coherence spectroscopy; mESC, mouse embryonic stem cell; MTS, (3-(4,5-dimethylthiazol-2-yl)-5-(3-carboxymethoxyphenyl)-2-(4-sulfo-phenyl)-2*H*-tetrazolium), NAD, nicotinamide adenine dinucleotide; NMR, nuclear magnetic resonance; NuMA, nuclear mitotic apparatus protein; PARP, poly(ADP-ribose)polymerase; PEG, poly(ethyleneglycol); THF, tetra-hydrofuran; TRF1, telomere repeat binding factor 1; TNKS, tankyrase.

selectivity towards TNKSs. Co-crystal structures of selected compounds with TNKS-2 revealed that the protein around the 8-position is more hydrophobic in TNKS-2 compared to PARP-1/2, rationalising the selectivity. The NAD^+-binding site contains a hydrophobic cavity which accommodates the 2-aryl group; in TNKS-2, this has a tunnel to the exterior but the cavity is closed in PARP-1. 8-Methyl-2-(4-trifluoromethylphenyl)quinazolin-4-one was identified as a potent and selective inhibitor of TNKSs and Wnt signalling. This compound and analogues could serve as molecular probes to study proliferative signalling and for development of inhibitors of TNKSs as drugs.

1. Introduction

Tankyrases (TNKSs) are members of the poly(ADP-ribose)polymerase (PARP) family of enzymes responsible for poly(ADP-ribosyl)ating acceptor proteins, using NAD^+ as a substrate [1]. TNKS-1 (PARP-5a, ARTD5) was first reported in 1998, being located at telomeres [2]. A closely-related isoform, TNKS-2 (PARP-5b, ARTD6), was first reported in 2001 [3]. TNKS-1 poly(ADP-ribosyl)ates telomere repeating binding factor (TRF1) and itself in order to regulate the elongation of telomeres [4-6]. TNKS-1 is essential for the correct structure and function of the mitotic spindle and centrosome through poly(ADP-ribosyl)ation of nuclear mitotic apparatus protein (NuMA) [7-9]. TNKS-1 is also involved in the glucose transport system [10,11]. It has a regulatory role in the life cycle of viruses, such as Epstein-Barr virus and Herpes simplex virus [12,13]. Aberrant Wnt signalling is found in the majority of colon cancers [14]. Tankyrase-1/2 is a component of the Wnt pathway, where it poly(ADP-ribosyl)ates Axin [14]. Inhibition of TNKSs causes stabilisation of Axin and degradation of β-catenin, thus decreasing nuclear β-catenin and inhibiting Wnt / β-catenin-driven proliferation of cancer cells [14]. Increased nuclear accumulation of β-catenin is found in many tumours [15-19] and inhibition of TNKS and Wnt signalling leads to antitumour activity *in vivo* [20,21]. Tankyrases are over-expressed in several clinical cancers and cancer cell lines, compared with the corresponding normal tissue / cell type. These tumours include breast cancer [4,22], colon cancer [23,24], chronic myeloid leukaemia [25], brain tumours [26,27], gastric cancers [28] and bladder cancers [29], pointing to one or more critical roles for the TNKSs in various tumour types.

Two binding sub-sites within the NAD^+-binding site have been identified and targeted for the design and evaluation of TNKS inhibitors. One sub-site normally binds the nicotinamide part of NAD^+ using the classical PARP motif though H-bonding to Ser1068 and Gly1032 and π-stacking interactions with Tyr1071 (TNKS-2 numbering). Several of the known inhibitors of the TNKSs bind here, including flavones **1** [30], 3-arylisoquinolin-1-ones **2** [31] and aryltetrahydronaphthyridinones **3** (Figure 1) [32]. In addition, 2-arylquinazolin-4-one **4**, containing a large and hydrophobic 4'-*tert*butylphenyl group, binds with the same conformation as **1**-**3** and is a potent inhibitor of TNKSs [33]. These interactions are also seen for XAV939 **5**, an extensively studied early inhibitor of the TNKSs [34]. IWR-1 **6** binds exclusively to the adenosine-binding site *via* induction of conformational change of specific amino-acid residues and does not interact with the nicotinamide-binding site [35]. IWR-1 **6** has been used as a scaffold towards the design and evaluation of additional inhibitors that bind to the adenosine-binding site, such as the oxazolidinone derivative **7** [36,37] and WIKI-4 **8** [38]. There is 83% overall sequence homology between TNKS-1 and TNKS-2 and 94% sequence homology between TNKS-1 and TNKS-2 at the catalytic domain; structures of both domains have been solved. In many circumstances, these isoforms perform their biomolecular functions redundantly [39].

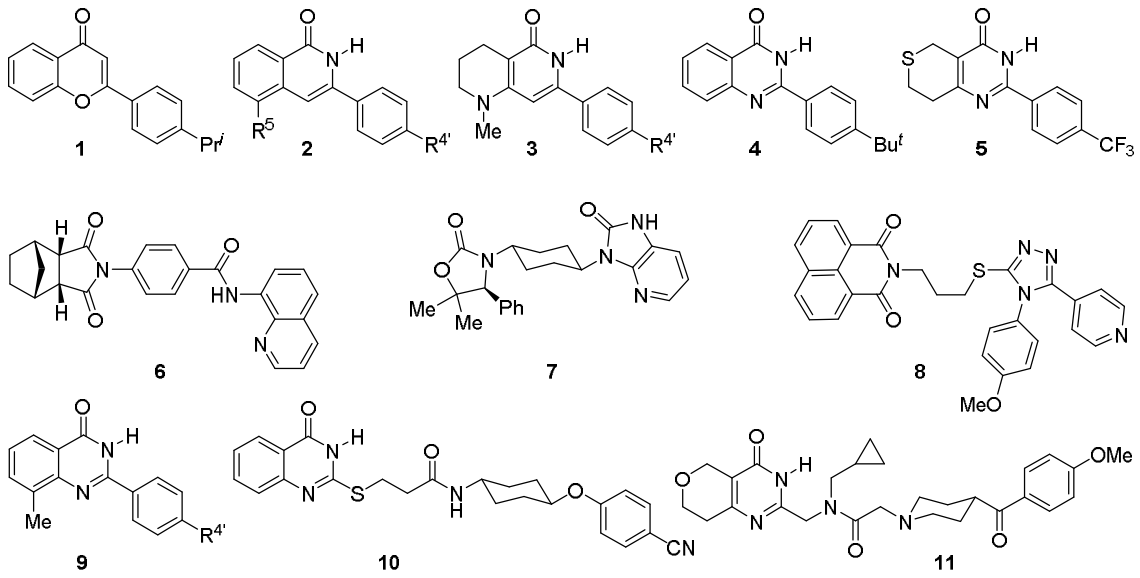

Figure 1. Structures of **1**-**11**, reported inhibitors of tankyrases.

In a preliminary communication, we previously disclosed a set of 8-methyl-2-arylquinazolin-4-ones **9** that bind to the nicotinamide-binding site [40]. The binding modes of these compounds were rationalised using modelling *in silico* that indicated specific tolerances around the 2-arylquinazolin-4-one scaffold. Compounds such as **4**, **6** and **9** were used to design dual-binding inhibitors that are capable of binding to the nicotinamide-binding site as well as interacting with the adenosine-binding site; these include **10** and **11** [41,42]. Although our preliminary study provided some initial information regarding Structure-Activity Relationships (SARs) of quinazolin-4-ones, to date, a comprehensive study into the SAR around the 4'- and 8-positions of the quinazolin-4-one scaffold and correlation with inhibition of TNKSs has not been performed. Here, we report the evaluation of our extended library of 2-arylquinazolinones with various groups at the 8-position, as well as a detailed assessment of hydrophobic, hydrophilic, electron-withdrawing, electron-neutral and electron-donating groups at the 4'-position. Counter-screening against PARP-1 and PARP-2 measured selectivity. Crystallographic studies rationalise the binding mode of these molecules, with particular attention to the nature of the 8-substituent. They reveal that 4'-groups which are hydrophobic and / or electron-withdrawing (Me, Br, Cl, CF_3) are optimal for potent and selective inhibition of the TNKSs compared to their activity against PARP-1 and PARP-2. To validate the activity of these novel compounds as inhibitors of potential active oncogenic Wnt signalling, a mouse embryonic stem cell (mESC) Wnt reporter assay was used. Our studies reveal that 8-methyl-2-(4-trifluoromethylphenyl)quinazolin-4-one **18c** is a potent and selective inhibitor of the TNKSs and Wnt signalling.

2. Results and Discussion

2.1. Chemical synthesis

Building on our original preliminary communication [40], we set out to prepare an extensive library of compounds, using a rational drug design approach, to assess the correlations between varying the 4'-group carried on the 2-phenyl ring and substitutions at the -6, -7 and -8 positions of the quinazolin-4-one scaffold with inhibition of TNKSs. The synthesis of quinazolin-4-ones used classical methods. 8-Unsubstituted 2-arylquinazolin-4-ones **13a-g,i** were synthesised in moderate yields using one-pot condensation of anthranilamide **12** with various 4-substituted

benzaldehyde derivatives, in the presence of hydrogensulfite ion, with *in situ* atmospheric oxidation of the intermediate aminal (Scheme 1). Reduction of the aromatic nitro group was achieved by transfer hydrogenation of **13g** to provide the aniline **13h**. The 4'-methoxyphenyl group of **13i** was demethylated to furnish the corresponding phenol in **13j**. In this series, the need for a lactam motif was tested with the simple amides **14**. Acylation of **12** with various 4-substituted benzoyl chlorides gave **14a-g,i**. Transfer hydrogenation of **14g** gave the aniline contained in **14h** but attempted selective demethylation of **14i** failed.

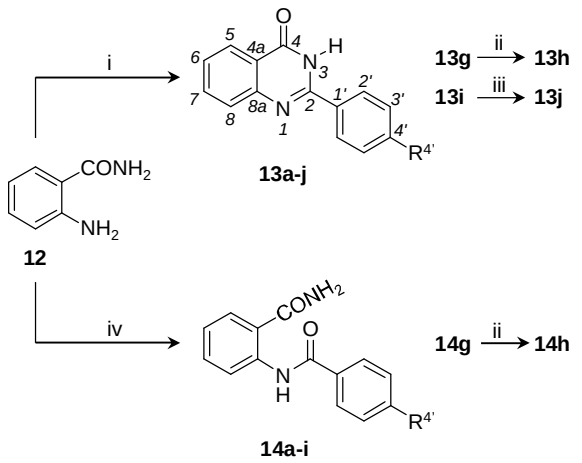

a: $R^{4'}$ = H; **b**: $R^{4'}$ = Me; **c**: $R^{4'}$ = CF_3; **d**: $R^{4'}$ = Cl; **e**: $R^{4'}$ = Br; **f**: $R^{4'}$ = F; **g**: $R^{4'}$ = NO_2; **h**: $R^{4'}$ = NH_2; **i**: $R^{4'}$ = OMe; **j**: $R^{4'}$ = OH

Scheme 1. Synthesis of 2-arylquinazolin-4-ones **13a-j** and acylated anthranilamides **14a-i**. *Reagents and conditions*: i, ArCHO, $NaHCO_3$, $AcNMe_2$, 150°C, open flask; ii, $^+NH_4HCO_2^-$, Pd/C, MeOH, DMF; iii, BBr_3, CH_2Cl_2, reflux, then NaOH; iv, ArCOCl, pyridine, dry THF.

Treatment of **15a,b** with 1,1'-carbonyldiimidazole at elevated temperatures formed the intermediates (*N*-acylimidazoles or isatoic anhydrides) which were treated with aqueous ammonia to give **16a,b** in good yields. Carbodiimide (EDC) activation and subsequent treatment with aqueous ammonia also provided **16a,b** in excellent yields [43,44]. The conversion of **16a** to **17** and **18** has been briefly described previously [40]. Acylation of 3-methoxyanthranilamide **16b** with 4-substituted benzoyl chlorides provided **19a-g,i**. The 4'-nitro group of **19g** was reduced to the corresponding amine using transfer hydrogenation conditions as before. Cyclisation of **19a-g,i** under strongly basic aqueous conditions (NaOH) gave **20a-g,i** in high yields. Dilute reaction mixtures and elevated temperatures were used to provide efficient cyclisation under basic conditions to the desired products.

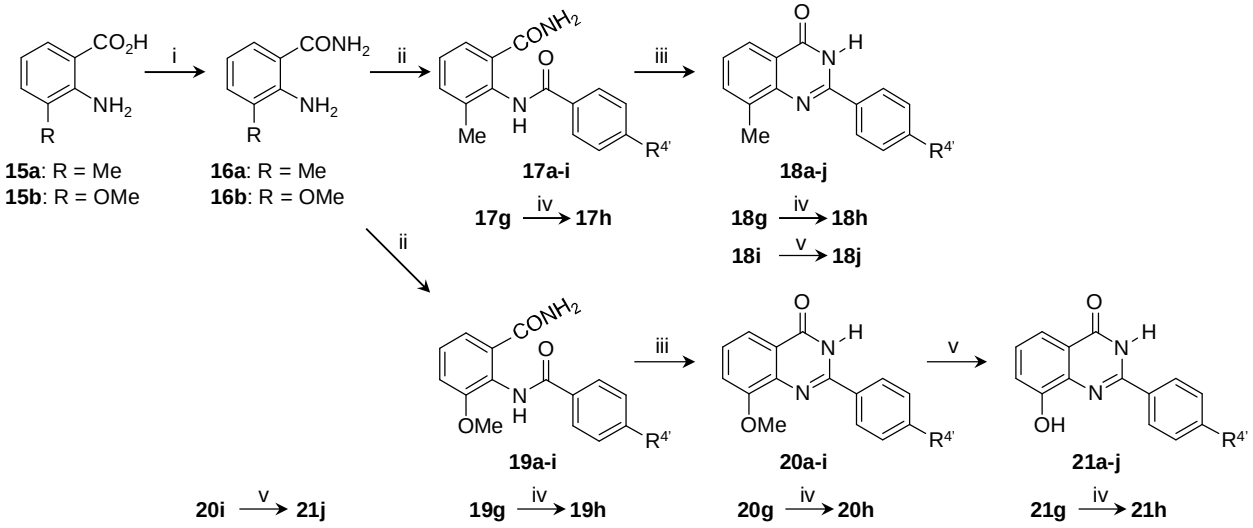

a: $R^{4'}$ = H; **b**: $R^{4'}$ = Me; **c**: $R^{4'}$ = CF_3; **d**: $R^{4'}$ = Cl; **e**: $R^{4'}$ = Br; **f**: $R^{4'}$ = F; **g**: $R^{4'}$ = NO_2; **h**: $R^{4'}$ = NH_2; **i**: $R^{4'}$ = OMe; **j**: $R^{4'}$ = OH

Scheme 2. Synthesis of 2-arylquinazolin-4-ones **18,20,21** with various 4'- and 8-substituents. *Reagents and conditions*: i, CDI or EDC, aq. NH_3, DMF; ii, ArCOCl, pyridine, dry THF; iii, aq. NaOH (0.5 M), 60 °C; iv, $^+NH_4HCO_2^-$, Pd/C, MeOH, DMF; v, BBr_3, CH_2Cl_2, reflux, then NaOH.

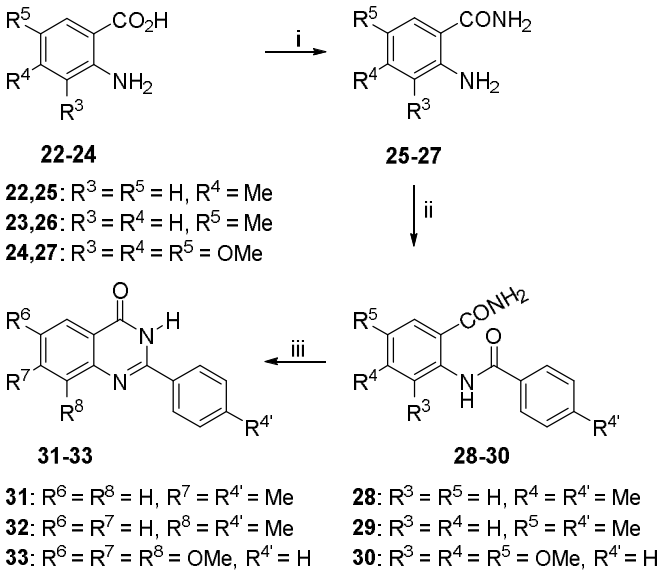

Scheme 3. Synthesis of 6- and 7-substituted 2-arylquinazolin-4-ones **31-33**. *Reagents and conditions*: i, CDI, aq. NH_3; ii, ArCOCl, pyridine, dry THF; iii, aq. NaOH (0.5 M).

Transfer hydrogenation was employed, as before, to reduce the nitro group of **20g** to the aniline in **20h**. Demethylation of **20a-g** using BBr_3 provided **21a-g** in satisfactory yields. Transfer hydrogenation of the nitro group in **21g** gave **21h**. Simultaneous demethylation of the 8- and 4'-methoxy groups of **20i** gave the corresponding diol **21j**.

Previous studies *in silico* suggested that substituents may not be tolerated at the 6- and 7-positions of the quinazolinone core. To test this experimentally, we prepared **31** and **32**, which are regioisomers of **18b**. The 6,7,8-trimethoxyquinazolinone **33** was also a target in this part of the study to assess whether a trisubstituted quinazolin-4-one would retain significant inhibitory activity towards the TNKSs. Briefly, formation of the primary amides from anthranilic acids **22-24** *via* EDC activation and treatment with aqueous ammonia gave **25-27**. Compounds **25,26** were acylated with 4-methylbenzoyl chloride to give the amides **28,29**. Amide **27** was acylated with benzoyl chloride to give **30**, after which **28-30** were cyclised under the usual aqueous basic conditions to provide **31-33**.

Compound **39**, which contains a CH_2NHCbz extension at the 4'-position, was shown in our preliminary study to retain good inhibitory activity against both TNKSs [40]. The extension is predicted by studies *in silico* to extend through the tunnel from the hydrophobic cavity to the exterior, where the aromatic ring of the Cbz may interact with the adenosine-binding site. To evaluate whether the presence of a 8-methyl substituent on the quinazolinone makes a significant contribution to binding in the presence of the CH_2NHCbz 4'-extension, analogue **38**, lacking the 8-Me group, was prepared along with the related 6,7,8-trimethoxy derivative **40** (Scheme 4). 4-(Aminomethyl)benzoic acid **34** was acylated with benzyl chloroformate under Schotten-Baumann conditions [45] before formation of the acid chloride. Subsequent coupling with anthranilamides **12, 16a, 27** gave **35-37**, respectively. Attempted cyclisation of **35-37** with aqueous sodium hydroxide led to hydrolysis of the carbamate; therefore, milder, less nucleophilic, basic conditions (aq. K_2CO_3) gave **38-40**. The Cbz units were removed by treatment with HBr, revealing the respective primary amines **41-43** as their hydrobromide salts, to test the tolerability of a polar charged moiety in the tunnel.

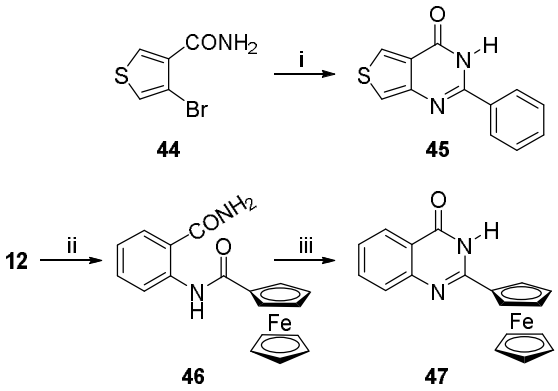

Scheme 5. Synthesis of thienopyrimidinone **45** and ferrocenylquinazolin-4-one **47**. *Reagents and conditions*: i, K_2CO_3, CuBr, $BnNH_2$, 125°C, DMSO, open flask; ii, ferrocenecarbonyl chloride, pyridine, dry THF; iii, aq. NaOH (0.5 M), 100°C.

Replacement of a benzene ring with thiophene is often considered as a conservative manipulation in drug design. This replacement was tested in the current series by synthesising and evaluating the thienopyrimidinone **45**. We have previously reported the synthesis of **45** in seven steps from dimethyl 3-thiahexanedioate in 3.5% overall yield [46]. With the new commercial availability of the aminothiophenecarboxamide **44**, we were able to prepare **45** in one step (Scheme 5). A Cu-catalysed displacement of the bromine with benzylamine, with oxidative cyclisation *in situ*, afforded the target in 16% yield. The ferrocene derivative **47** was assembled to evaluate the possibility of accommodating three-dimensional bulk into the hydrophobic pocket of TNKSs. Compound **47** was prepared in the usual way (Scheme 5) by acylation of anthranilamide **12** with ferrocenecarbonyl chloride, followed by cyclisation of intermediate **46** with under aqueous basic conditions.

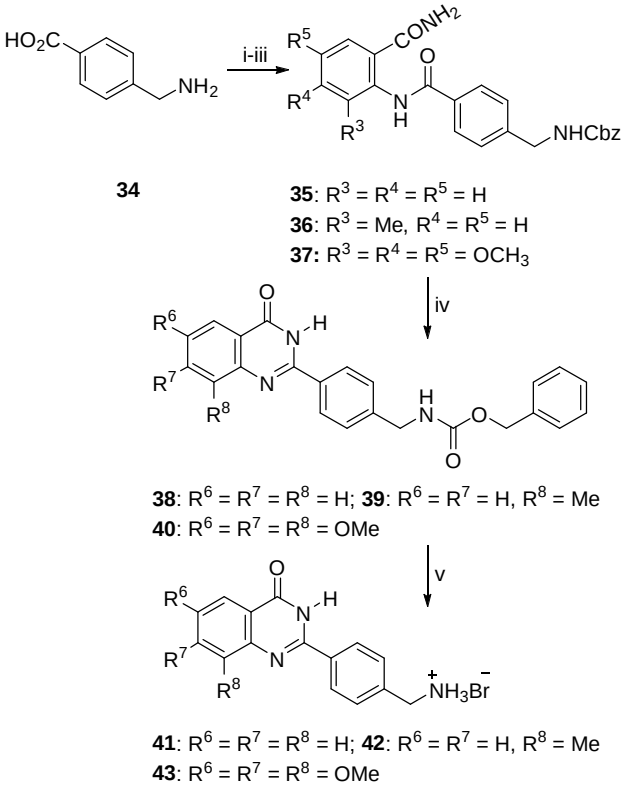

Scheme 4. Synthesis of 2-arylquinazolin-4-ones **38-43** with extensions at the 4'-position. *Reagents and conditions*: i, CbzCl, aq. K_2CO_3; ii, $SOCl_2$, iii, **12** or **16a** or **27,** pyridine, dry THF; iv, aq. K_2CO_3 (1.0 M), 100°C; v, HBr, AcOH.

Table 1. Inhibition of TNKS-1, TNKS-2, PARP-1 and PARP-2 by 8-H 2-arylquinazolin-4-ones **13**. IC_{50} values in nM.

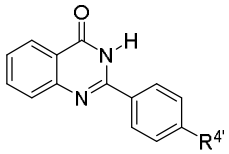

Cpd.	$R^{4'}$	TNKS-1	TNKS-2	PARP-1	PARP-2
XAV939 **5**		10 ± 3	17 ± 6	1200 ± 23	
13a	H	1406 ± 156	2200 ± 32	2863 ± 1753	
13b	Me	346 ± 25	540 ± 195	424 ± 215	
13c	CF_3	425 ± 177	133 ± 82	>100000[a]	>10000[a]
13d	Cl	485 ± 50	54 ± 4	>100000[a]	2600 ± 124
13e	Br	224 ± 49	101 ± 29	>100000[a]	>100000[a]
13f	F	781 ± 125	1102 ± 95	>100000[a]	4688 ± 918
13g	NO_2	1100 ± 49	259 ± 125	>10000[a]	2064 ± 108
13h	NH_2	786 ± 162	690 ± 160	1295 ± 121	
13i	OMe	250 ± 70	611 ± 125	2718 ± 1846	
13j	OH	528 ± 76	189 ± 50	6429 ± 769	
38	CH_2NHCbz	2423 ± 1825	45 ± 24	>10000[a]	>10000[a]

[a] Limited by solubility.

2.2. Potency and selectivity of inhibition of tankyrases

An initial screen of the inhibitory activity of all test compounds was performed using three different concentrations of inhibitor using our previously developed assay, which uses an immobilised construct of the catalytic and SAM domains of TNKS-2 [40]. Values are expressed as percentage inhibition of enzyme activity relative to control containing no inhibitor (see Supplementary Information). From this initial screen, compounds that diminished enzyme activity by >60% at 1.0 µM were evaluated further to determine IC_{50} values against TNKS-1, TNKS-2 and, for counter-screening, PARP-1. Compounds that showed good selectivity of inhibition of TNKSs, compared to PARP-1, were also assessed against PARP-2.

Benzamides **14a-i**, **17a-h**, **19a-h**, **35** and **36** were evaluated against TNKS-2 at 1.0 µM, 100 nM and 10 nM (Supplementary Information) to assess the importance of the lactam and its constraint of the conformation of the H-bond motif, which makes interactions with Glu1138 and Ser1068 [32]. ^{1}H NMR data suggest that the primary amide in these compounds is coplanar with the benzene ring but rotated 180° relative to its conformation in the quinazolinones (Figure 2). Compounds **14a-i**, **17a-h**, **19a-h**, **35** and **36** displayed poor inhibition towards TNKS-2 at 1.0 µM and, therefore, were not evaluated further. It is thus important that the lactam ring is fixed to potentiate inhibitory activity towards TNKSs.

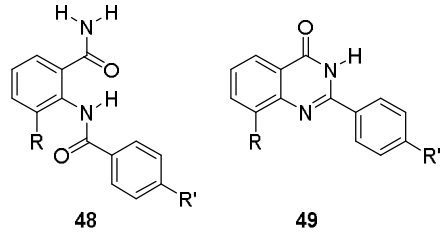

Figure 2. Conformations of aroylanthranilamides **48** and 2-arylquinazolinones **49** in solution.

Table 2. Inhibition of TNKS-1, TNKS-2, PARP-1 and PARP-2 by 8-OMe 2-arylquinazolin-4-ones **20**. IC_{50} values in nM.

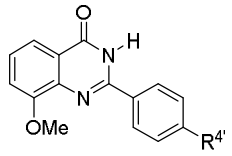

Cpd.	$R^{4'}$	TNKS-1	TNKS-2	PARP-1	PARP-2
20a	H	475 ± 12	1029 ± 235	>10000[a]	1539 ± 238
20b	Me	153 ± 12	167 ± 60	2404 ± 575	
20c	CF_3	73 ± 2	87 ± 34	>100000[a]	570 ± 25
20d	Cl	155 ± 55	62 ± 11	>10000[a]	6022 ± 1107
20e	Br	111 ± 5	106 ± 23	>100000[a]	259 ± 84
20f	F	299 ± 74	459 ± 166	>10000[a]	1562 ± 85
20g	NO_2	873 ± 334	863 ± 221	>10000[a]	928 ± 46
20h	NH_2	1284 ± 234	1076 ± 158	1589 ± 114	
20i	OMe	346 ± 25	128 ± 27	1244 ± 29	

[a] Limited by solubility.

The 2-arylquinazolin-4-one derivative **31**, bearing a methyl group at the 7-position, showed weak inhibition against TNKS-2 (18% at 1.0 μM; see Supplementary Information). Compound **32** bearing a 6-methyl group also displayed weak inhibition of TNKS-2 (10% at 1.0 μM). Previous studies *in silico*, accompanied by analysis of the TNKS-2–**5** bioactive conformation (PDB code 3KR8), revealed that substituents in the 7- or 6-positions may be tolerated *via* potential interaction with Glu^{1138} but the hydrophobic Me would not allow this.

In our preliminary communication, we reported that a charged primary amine was not tolerated at the junction of the hydro-phobic cavity and the tunnel, in that **42** (carrying 4'-$CH_2N^+H_3$) was much less active as an inhibitor of TNKS-2 than was the corresponding 4'-Me compound **18b** [40]. By contrast, more lipophilic charged tertiary amines are tolerated in this position in the 3-arylisoquinolin-1-one series [31]. The deleterious effect of the charged polar 4'-$CH_2N^+H_3$ in the present 2-arylquinazolin-4-one series was confirmed by the minimal inhibition of TNKS-2 by the 8-H analogue **41** at 1.0 μM and by the complete inactivity of **43** at this concentration.

The data for inhibition of the enzymes by the 8-H quinazolinones **13a-j** are shown in Table 1. In this series, compounds **13c** (4'-CF_3), **13d** (4'-Cl) and **13e** (4'-Br), which carry lipophilic groups on the 2-phenyl ring, demonstrate good inhibition of TNKS-1 and TNKS-2; good isoform-selectivity was noted, with only weak activity against PARP-1 and PARP-2. Curiously, the 4'-Me analogue **13b** showed no isoform-selectivity whatsoever, being a good inhibitor of PARP-1 (IC_{50} = 424 nM). Slightly weaker activity against the tankyrases was demonstrated by **13h-j**, which carry hydrophilic and / or electron-donating substituents at the 4'-position; these compounds also showed some inhibition of PARP-1, leading to lower selectivity than **13c-e**. Small substituents (H, F) at the 4'-position in **13a,f** lead to lower activity against the tankyrases and greater affinity for PARP-1. The planar –M nitro group in **13g** gives weaker activity against TNKS-1 but increased affinity for PARP-2, giving lower selectivity. In

this 8-H quinazolinone series, optimum activity and selectivity is seen for non-polar units at the 4'-position. However, the extended $–CH_2NHCbz$ at the 4'-position in **38** provided remarkable selectivity for the TNKS-2 isoform over TNKS-1, PARP-1 and PARP-2.

Table 3. Inhibition of TNKS-1, TNKS-2, PARP-1 and PARP-2 by 8-OH 2-arylquinazolin-4-ones **21**. IC_{50} values in nM.

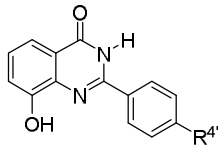

Cpd.	R4'	TNKS-1	TNKS-2	PARP-1
21a	H	195 ± 21	180 ± 94	1034 ± 116
21b	Me	22 ± 2	44 ± 6	559 ± 34
21c	CF_3	53 ± 11	25 ± 1	3105 ± 172
21d	Cl	46 ± 12	49 ± 14	645 ± 221
21e	Br	47 ± 3	15 ± 1	130 ± 40
21f	F	101 ± 39	263 ± 134	1361 ± 608
21g	NO_2	58 ± 23	191 ± 52	105 ± 5
21h	NH_2	83 ± 18	219 ± 51	289 ± 135
21j	OH	156 ± 28	86 ± 10	856 ± 137

[a] Limited by solubility.

Changing the 8-substituent from 8-H to 8-OMe (Table 2 **20a-i**) provided an overall increase of potency of inhibition of tankyrases, compared to **13a-j**. The nature of the 4'-group for compounds **20a-i** shows similar SAR as for **13a-j**. Large and electron-withdrawing groups (**20c-g**) provide potent and selective inhibition of TNKS. Again, in this series (Table 2), selective inhibition of TNKS is observed with small electron-withdrawing 4'-groups (4'-F in **20f**) then small neutral groups (4'-H in **20a**), when comparing inhibition values against those for PARP-1. However, in this series, the presence of an electron-donating 8-OMe group provides a notable increase in inhibitory potency against PARP-2. For example, **20c,e,g** show sub-micromolar inhibition of PARP-2, giving poor selectivity of inhibition of the target tankyrases. However, these compounds may represent a new starting-point for the design of PARP-2-selective inhibitors, with **20e** showing >300-fold selectivity for PARP-2 over PARP-1. It is notable that previously reported selective inhibitors of PARP-2 were claimed to have selectivity of only *ca*. 50-fold (for 5-benzoyloxyisoquinolin-1-one) [48], which could not be repeated by other workers who demonstrated *ca*. 11-fold selectivity for the optimum compound 5-benzamidoisoquinolin-1-one in a comparative study [49,50].

The presence of an electron-donating / hydrophilic 8-OH group (**21a-i**, Table 3) provides more potency towards TNKS, compared to **13a-j** (8-H), whereas the IC_{50} values are broadly similar to those for **20a-i** (8-OMe). However, the introduction of this polar group in **13a-j** significantly enhances binding to PARP-1, leading to lower selectivity. As inhibitors **21a-i** showed poor selectivity *vs*. PARP-1, they were not evaluated further against PARP-2. In this series, large (Cl, Br) and electron-withdrawing groups (F, CF_3, NO_2) provided more potent inhibition of TNKSs, compared to those bearing small 4'-substituents, an observation that mirrors those observed for compounds presented in Tables 1 and 2. Interestingly, compound **21**, presenting an 8-OH substituent, had much greater antiproliferative activity against HT29 human colon carcinoma cells (see Supplementary Information), compared to all other quinazolin-4-ones examined. One may speculate whether a requirement for concurrent inhibition of TNKSs and PARP-1 may be required to achieve this activity in HT29 colon cancer cells or that the compounds may be taken up into the cells more effectively. However, the observation that the 8-Me compound **18c** is capable of inhibiting Wnt signalling in cells (see below) suggests that this series can be taken up into cells readily.

The inhibitory activities of **18a-j, 39** and **42** (8-Me, Table 4) against TNKS-1, TNKS-2 and PARP-1 were reported in our preliminary communication [40] and are provided for comparison. Compounds that did not display PARP-1 inhibitory activity up to 5000 nM have now been further assessed for PARP-2 inhibition to assess their isoform-selectivity further. Inhibition of PARP-2 by these compounds was broadly similar to inhibition of PARP-1 but with somewhat lower IC_{50} values. The excellent isoform selectivity for TNKSs *vs.* other PARPs is further confirmed.

The quinazolinone core was changed to thieno[3,4-*d*]pyrimidin-4(3*H*)-one in **45**. The 7-position of **45** is unsubstituted, so comparison with **13a** is apposite. The activities of **45** against the isoforms are slightly greater (IC_{50} *vs.* TNKS-1 = 466 ± 11 nM, IC_{50} *vs.* TNKS-2 = 2455 ± 123 nM, IC_{50} *vs.* PARP-1 = >10000 nM, IC_{50} *vs.* PARP-2 = 11500 ± 225 nM), reflecting the conservatism of the benzene-to-thiophene replacement. However, **45** is much less potent than XAV939 **5** against the tankyrases (Table 1), showing the importance of the flexibility of the tetrahydrothiapyran in **5**. The ferrocenylquinazolin-4-one **47** displayed weak inhibition of the TNKSs (IC_{50} *vs.*TNKS-1 = 1217 ± 28 nM , IC_{50} *vs.* TNKS-2 = 4589 ± 966 nM); weaker binding to PARP-1 was noted (IC_{50} >10 μM) but PARP-2 was inhibited with IC_{50} = 1600 ± 114 nM). Similar activity has been reported previously by us for 3-ferrocenyl-5-methylisoquinolin-1-one [31]. These data show that the hydrophobic pocket in the tankyrases is capable of accepting some 3-D bulk.

Table 4. Inhibition of TNKS-1, TNKS-2, PARP-1 and PARP-2 by 8-OH 2-arylquinazolin-4-ones **18**. IC_{50} values in nM.

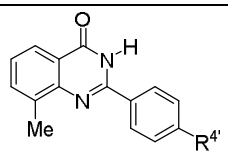

Cpd.	$R^{4'}$	TNKS-1	TNKS-2	PARP-1	PARP-2
18a	H	41 ± 18[a]	42 ± 18[a]	795 ± 48[a]	
18b	Me	35 ± 12[a]	7 ± 2[a]	685 ± 89[a]	
18c	CF_3	48 ± 7[a]	10 ± 3[a]	>5000[a,b]	3098 ± 1524
18d	Cl	36 ± 4[a]	33 ± 7[a]	>5000[a,b]	6350 ± 704
18e	Br	32 ± 4[a]	6 ± 1[a]	>5000[a,b]	10529 ± 3322
18f	F	44 ± 13[a]	40 ± 8[a]	>5000[a,b]	683 ± 15
18g	NO_2	32 ± 8[a]	30 ± 14[a]	104 ± 46[a]	
18h	NH_2	35 ± 10[a]	3 ± 1[a]	504 ± 128[a]	
18i	OMe	37 ± 7[a]	12 ± 4[a]	891 ± 142[a]	
18j	OH	52 ± 11[a]	6 ± 1[a]	1200 ± 160[a]	
39	CH_2NHCbz	44 ± 4[a]	73 ± 28[a]	>5000[a,b]	>100000[b]
42	$CH_2N^+H_3\ Br^-$	907 ± 26	43 ± 13	266 ± 19	

[a] Determined previously [40]. [b] Limited by solubility.

Several SAR themes are evident from this comprehensive study. Firstly, the hydrophobic 8-Me group provides increased potency, compared to 8-H, 8-OMe and 8-OH, regardless of the nature of the 4'-substituent. The SAR at the 4'-substituent for the 8-Me in **18a-j** is comparable to those in this region in **13a-j, 20a-i** and **21a-h,j**, where large and electron-withdrawing 4'-groups are required for potent TNKS inhibition. Again, small 4'-electron-withdrawing groups (4'-F in **18f**) provides similar potency against TNKSs as compounds bearing small 4'-neutral groups (4'-H in **18a**). However, as with **13f, 20f** and **21f** (all 4'-F), **18f** provides selective inhibition of TNKSs compared to their respective 4'-H counterparts. Compound **18e**, containing a large 4'-Br, is the most potent and selective TNKS inhibitor in this series. The 4'-extended Cbz group of **39** retains selective inhibition towards TNKSs over PARP-1/-2.

2.3. Structural studies

To rationalise SARs displayed in Tables 1-4, selected compounds were co-crystallised with the catalytic domain of TNKS-2. The structures of nine compounds (**13b, 13c, 18b, 18c, 20b, 20c, 21b, 21c** and **38**) in complex with this construct were solved at 1.7 to 2.4 Å resolution (Figure 3), varying the 8-substituent but maintaining the 4'-group as either 4'-methyl (**13b, 18b, 20b, 21b**) or 4'-trifluoromethyl (**13c, 18c, 20c, 21c**). In all cases, the quinazolin-4-one scaffold binds into the nicotinamide-binding site forming the usual conserved interactions. The lactam N-H forms a hydrogen bond to the backbone carbonyl of Gly^{1032}, whilst the C=O of the lactam forms two hydrogen bonds to the backbone C=O of Gly^{1032} and the hydroxy side chain of Ser^{1068}. The quinazolinone / lactam ring creates π-stacking interactions with Tyr^{1071}. The hydrophobic cavity, lined with Tyr^{1050}, Ile^{1075}, Pro^{1034} and Phe^{1035}, can accommodate large groups at the 4'-position, including Br (**13e, 18e, 20e** and **21e**) and Cl (**13d, 18d, 20d** and **21d**). Compound **38**, which contains the extended 4'-$CH_2NHCO_2CH_2Ph$ interacts further with Pro^{1034} and Phe^{1035}, unlike the simpler quinazolinones. The binding of **38** does not cause large changes in the conformation of the protein (Figure 3 panel I) but there is some minor structural movement of the side-chain of Ile^{1075} as the backbone amide NH of Ile^{1075} makes a partial hydrogen bond (3.71 Å; not shown for clarity) to the benzyl oxygen of **38**. No additional or significant movement is observed for residues that are in close proximity to the large 4'-CH_2NHCbz group of **38** as it threads treads through the tunnel at the distal end of the hydrophobic cavity.

Selective inhibition of TNKSs over PARP-1 can be rationalised by structural alignment of the TNKS-2-**38** structure with a PARP-1 structure containing 8-hydroxy-2-methylquinazolin-4-one (PDB code 4PAX) (Figure 3, panel J). The two protein structures were aligned to overlap the nicotinamide-binding motifs and the structure of the ligand 8-hydroxy-2-methylquinazolin-4-one has been removed for clarity in the figures. Figure 3, panel J shows that the 2-aryl unit of **38** would cause steric clashes with a-helical residues Asn^{767}, Asp^{766} and Gln^{763} of PARP-1. Additionally, the cavity accommodating the 4'-carboxybenzyl group is in a closed state in PARP-1, whereas the corresponding region of protein in TNKS-2 is hydrophobic and open to solvent through the tunnel (Figure 3, panel I). The hydrophilic nature of this PARP-1 surface is, therefore, suited towards 2-arylquinazolin-4-one derivatives containing hydrophilic 4'-substituents (4'-NH_2 and 4'-OH). Conversely, this hydrophilic α-helical region in PARP-1 is

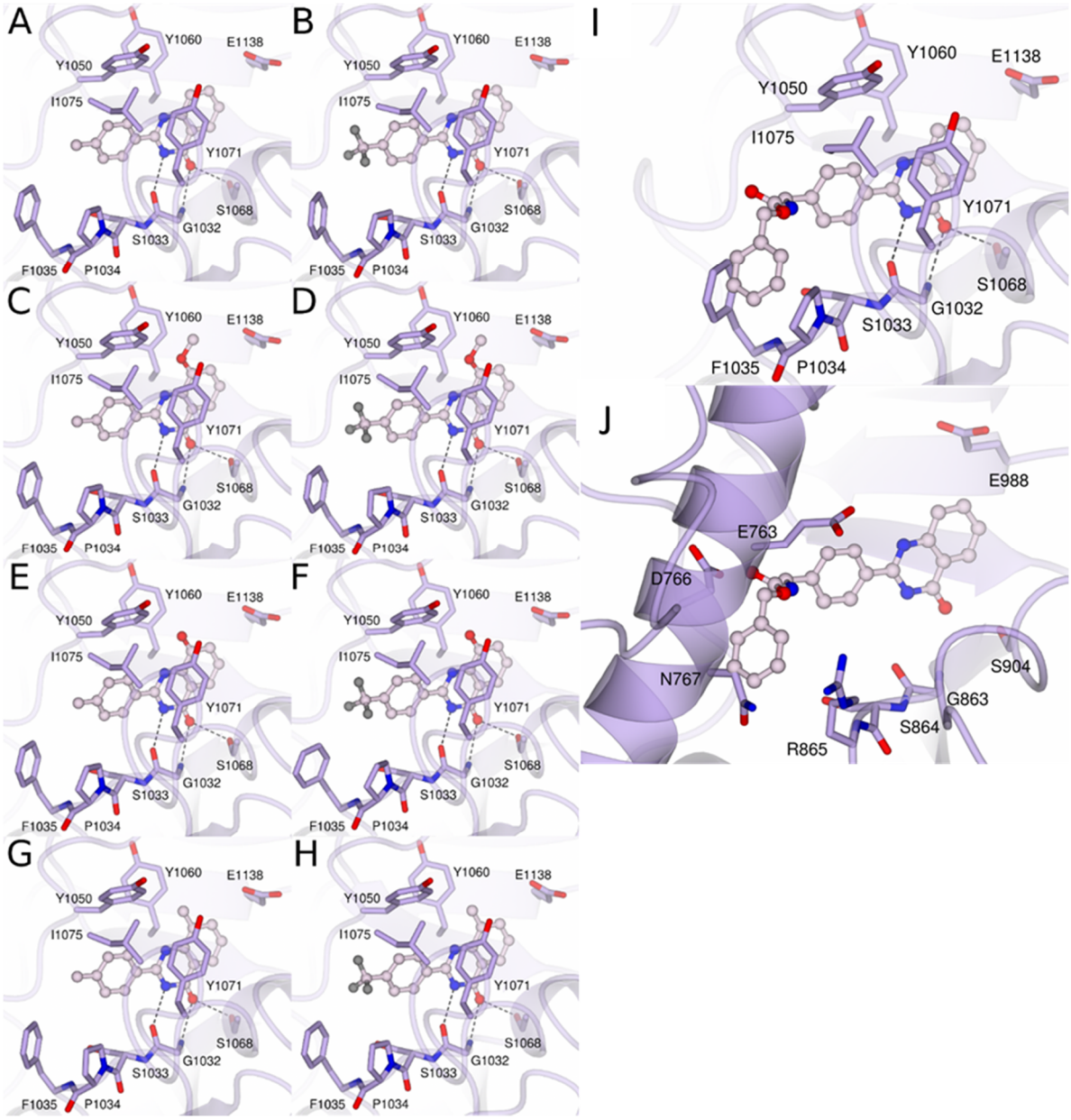

Figure 3. Crystal structures of Panel A **13b**, Panel B **13c**, Panel C **20b**, Panel D **20c**, Panel E **21b**, Panel F **21c**, Panel G **18b**, Panel H **18c**, Panel I **38** bound to TNKS-2. Overlay of **38** onto PARP-1 (panel J). Key residues are in purple and key H-bond interactions are shown as dashed lines.

intolerant of electronegative or large hydrophobic groups at the 4'-position, leading to greater selectivity of 2-arylquinazolinones carrying 4'-hydrophobic groups towards TNKS-1 and TNKS-2. The presence of a large, hydrophobic 4'-group causing potent TNKS inhibition has been observed using **4** [33]. A clear SAR at the 8-position was observed for inhibition of both TNKS-1 and TNKS-2: 8-Me > 8-OH > 8-OMe > 8-H. Similar SAR had been deduced earlier for the 3-arylisoquinolin-1-ones (5-Me > 5-OMe > 5-OH = 5-NH_2 = 5-F). Structural alignment of the PARP-1 (PDB code 4PAX) and TNKS-2-**38** crystal structures shows that a larger space around the 8-position is present in PARP-1 than in TNKS-2 (Figure 3). In addition, the corresponding hydrophobic residue Tyr^{1050} of TNKS-2 is absent from PARP-1. Glu^{988} in PARP-1 is 3 Å closer to the 8-position than the corresponding Glu^{1138} of TNKS-2. The closer proximity of

Glu988 and lack of a hydrophobic residue around the 8-position of the quinazolinone scaffold provides a more hydrophilic site in PARP-1, compared to TNKS-2, and may possibly explain why hydrophilic groups in the 8-position (such as 8-OH) is well tolerated in the PARP-1 binding site. The protein surrounding the 8-position of the quinazolinone scaffold in TNKS-2 is more hydrophobic in nature due to the presence of a proximal Tyr^{1050} and, therefore, a hydrophobic 8-Me group in **18a-j** provides improved inhibitory activity and selectivity towards TNKSs.

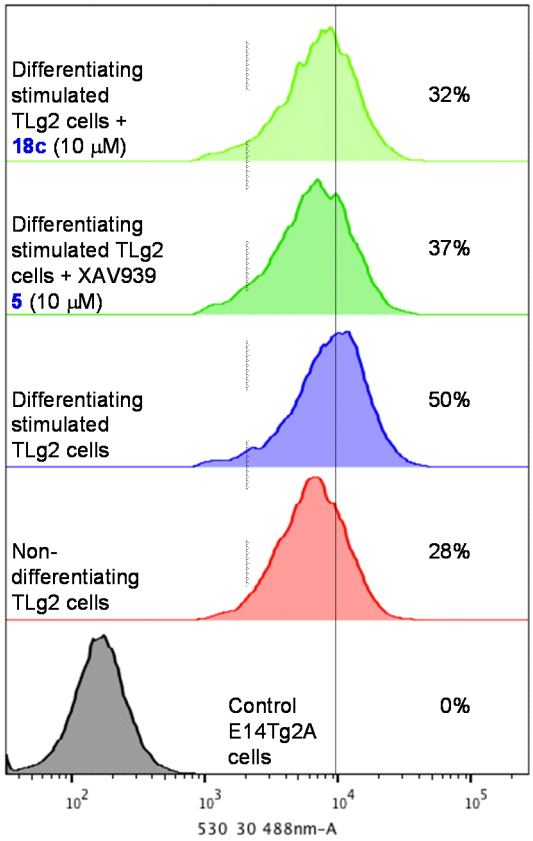

Figure 4. Flow-cytometric analysis of TLg2 cells (and E14Tg2A control cells) grown under the indicated culture conditions. The black line indicates the median GFP fluorescence intensity of TLg2 cells cultured for 3 d in the presence of N2B27 medium and % is the percentage of cells found with fluorescence above that level under the various conditions.

The TNKS-2 structure was solved with two molecules in the unit cell and, therefore, the numbers of water molecules in close proximity to the quinazolinone 8-position in both monomer chains A and B were considered. The number of water molecules in this area was averaged between the two chains. We measured the number and distance of water molecules that were within 6.5 Å of the 8-carbon of the quinazolinone scaffold for compounds **4b**, **10b**, **11b** and **12b**. There appears to be correlation between the amount and distance of water molecules and inhibitory activity of these compounds. This is particularly seen between compounds **4b** and **10b.** The presence of a total of six water molecules (three in each chain) for **4b** results in a ten-fold decrease in inhibitory activity, compared with **10b** which contains four water molecules (two in each chain) that are in proximity to C-8 of the compound. A combination of the hydrophobic nature of protein surrounding the 8-position in TNKS-1 and TNKS-2 (compared to PARP-1 which is more hydrophilic) and the amount of water repulsion in this region may provide an explanation why 8-Me is optimum for potency against TNKSs.

Most of the quinazolinones reported here were more potent towards PARP-2 than against PARP-1. XAV939 **5**, which also binds to the nicotinamide-binding site, was eight-fold more potent towards PARP-2 compared to PARP-1, which was consistent with literature values [33].

2.4. Inhibition of Wnt signalling

Inhibitors **5**, **18c**, **18d**, **18e**, **18f**, **20d**, **20c** and **39** displayed selective and potent TNKS inhibition and were investigated further to assess their cellular activity as inhibitors of the Wnt signalling cascade, using an established assay based on mouse embryonic stem cells (mESCs) [51,52]. In mESCs, canonical Wnt signalling is negligible and only becomes active as the cells differentiate [51,53,54]. As shown in Figure 4 (grey) and Table 5, E14Tg2A mESCs, which lack the green fluorescent protein (GFP) gene, showed minimal fluorescence. Derived TLg2

cells express a GFP reporter under the control of Wnt signalling. Under standard growth conditions, TLg2 cells do not differentiate and display basal levels of green fluorescence (Figure 4, pink; Table 5). When these cells are cultured in N2B27 medium for 3 d, they differentiate, there is an activation of the Wnt reporter and the median GFP fluorescence increases (from 6405 to 8894 units; Figure 4, blue; Table 5), as measured by flow cytometry [51]. Inhibitors of the Wnt response will lead to a decrease in the percentage of cells with fluorescence above this value (8894 units). The experiment was repeated in the presence of test quinazolinones **18c-f, 20c,d, 39** (10 mM) or XAV939 **5** (control, 10 mM).

Table 5. Summary of the results obtained after flow cytometry analysis in TLg2 cells cultured in the indicated culture conditions. E14Tg2A cells are a non-fluorescent control cell line.

Cell line	Culture condition	Median GFP fluorescence	% cells above the median GFP fluorescent intensity in cells under differentiation (N2B27)
E14Tg2A	0-3SL	1209	0
TLg2	0-3SL (standard)	6405	28
TLg2	N2B27 (differentiation)	8894	50
TLg2	N2B27 + XAV939 **5**	7424	37
TLg2	N2B27 + **18c**	6650	32

The positive control, XAV939 **5**, is known to inhibit Wnt signalling in a different model [14,51] and this effect was confirmed in our model by diminution to 37% of the proportion of cells with GFP fluorescence >8894 units (Figure 4, dark green; Table 5) (compared with 50% for no drug and 28% for non-differentiating controls). 8-Methyl-2-(4-trifluoromethylphenyl)quinazolin-4-one **18c** was shown to be more potent than **5** in this Wnt-inhibition assay, in that it reduced the proportion of cells with GFP fluorescence >8894 units to 32% (Figure 4, pale green; Table 5), very close to the basal non-differentiating level for these cells. These effects are also reflected in the diminution of the median fluorescence values (Table 5). Analogous quinazolinones **18d,e, 20c, 39** showed lesser inhibition of the Wnt response in this assay, while **18f, 20d** were effectively inactive. All the test quinazolinones were evaluated for antiproliferative activity against HT29 cells (see below and Supplementary Information). Inhibitor **18c** did not display any activity in this MTS cell proliferation assay, consistent with results shown using mESCs.

2.5. Antiproliferative activity

Compounds **13a-j**, **18a-j**, **20a-h**, **21a-h**, **39**, **42**, **45** and **47** were assessed for their antiproliferative / cytotoxic effects against HT29 human colon carcinoma cells using an MTS assay. Three concentrations of each compound were used (see Supplementary Information). Inhibitors **13j** and **18j** showed inhibition of of the proliferation of HT29 cells in a dose-dependent manner. These compounds maintain a 4'-OH substituent but differ at the 8-position (8-H and 8-Me, respectively) and display some PARP-1 inhibitory activity (IC_{50} = 6429 nM and IC_{50} = 1200 nM, respectively). Inhibitors **21a** (4'-H), **21b** (4'-Me), **21d** (4'-Cl), **21e** (4'-Br), **21h** (4'-NH_2) and **21j** (4'-OH) all carry a 8-OH group and are capable of inhibiting the TNKSs and PARP-1. Their enzyme-inhibitory activities may complement their observed concentration-dependent inhibition of proliferation of HT29 colon cancer cells. The observed correlation between dual TNKS-1/-2 and PARP-1 inhibitory activity and inhibition of HT29 cells is also demonstrated by **42**. We therefore speculate whether dual TNKS and PARP-1 inhibition may be necessary for antiproliferative activity against colon cancer cells. Alternatively, it may be that the limited

solubility of some analogues in the assay medium masked their antiproliferative effect by not allowing a sufficient concentration to be achieved. In general, we observed turbid solutions for the 8-Me, 8-OMe and 8-H series of compounds at 100 μM (see Supplementary Information). The 8-OH group of inhibitors **21a** (4'-H), **21b** (4'-Me), **21d** (4'-Cl), **21e** (4'-Br), **21h** (4'-NH_2) and **21j** (4'-OH) provides increased aqueous solubility, thus facilitating the observation of antiproliferative activity at 100 μM. Interestingly, potent and selective inhibitors of TNKSs, for example **18c** and **5**, did not inhibit proliferation of HT29 cells but do inhibit Wnt signalling.

3. Conclusions

In this study, the SAR around the 8- and 4'-positions in series of 2-arylquinazolin-4-ones has been explored for inhibition of the tankyrases and for activity against the isoforms PARP-1 and PARP-2. At the 8-position, a small hydrophobic group (methyl) gave the best potency for inhibition of both tankyrases and selectivity in the counter-screen against the isoforms PARP-1 and PARP-2. Conversely, a polar H-bond donor (8-OH) at this position caused some loss of potency against the tankyrases but considerably increased activity against PARP-1. These data were rationalised by modelling studies and by comparison of the crystal structures of complexes with TNKS-2 and the structure of PARP-1. It was evident that the protein surface in the region of space which accommodates the 8-substituent is much more polar in PARP-1 than it is in the tankyrases. This is the first detailed comparison of the binding sites in these related NAD^+-binding enzymes. The conclusions are consistent with our previous study of 3-arylisoquinolin-1-ones, where 5-NH_2 (equivalent to the 8-position in the quinazolinones) led to increased inhibition of PARP-1 and decreased inhibition of the tankyrases, in comparison with the 5-Me analogues. Substitution at the 6- and 7-positions of the quinazolinones is not tolerated. We had previously established that the optimum location for a substituent on the exocyclic phenyl ring is 4'- [31]. Examination of the surfaces of the binding pockets in this region for TNKS-2 and PARP-1 indicated that larger and more hydrophobic substituents would be accepted in the tankyrases and this proved to be the case experimentally. Selectivity for inhibition of tankyrases is seen for 4'-Cl and 4'-Br, hydrophobic substituents which interact well with the hydrophobic surface in tankyrases but not with the tighter hydrophilic surface in PARP-1. The 4'-CH_2NHCbz unit extends into a tunnel from the cavity towards solvent; this tunnel is lined by both hydrophobic and hydrophilic residues. Thus optimum potency and selectivity for inhibition of tankyrases by 2-arylquinazolin-4-ones is achieved with 8-methyl and 4'-hydrophobic groups.

8-Methyl-2-(4-trifluoromethylphenyl)quinazolin-4-one **18c** is identified by this comprehensive study as a highly potent and selective inhibitor of the tankyrases *in vitro* and in a functional cellular assay, with potential for further development as a molecular probe for further studies on the roles of the tankyrases. A panel of compounds with differing isoform-selectivities is now readily available as a tool for cellular studies on the interplay of the members of the PARP superfamily.

4. Experimental

4.1. Protein crystallography

Crystal structures of TNKS-2 were used to study the binding modes of the compounds. The catalytic domain of TNKS-2 was expressed, purified and crystallised as previously reported [39]. Inhibitors were soaked for 48 h into the crystals in a well solution (0.2 M $LiSO_4$, 0.1 M Tris-HCl pH 8.5, 24-26% PEG 3350) supplemented with the compound (100 μM) and 250 mM NaCl. Before collection of the data, the crystals were briefly soaked in a well solution

supplemented with 20% glycerol and flash frozen in liquid nitrogen. Data was collected at the Diamond Light Source (Didcot, UK) at beamlines I04-1 and I03 and at ESRF (Grenoble, France) at beamline ID23-2. Diffraction data were processed and scaled with the XDS package [55]. The structures were solved using the Difference Fourier method with the starting phases derived from the TNKS-2 structure (PDB accession code 3U9H). REFMAC5 [56] was used for refinement and COOT [57] for manual building of the model. Data collection and refinement statistics are shown in the Supporting Information. Coordinates and structure factors have been deposited into the RCSB Protein Data Bank (http://www.rcsb.org) with the following accession codes: 4UHG, 4UI3, 4UI5, 4UI6, 4UI7, 4UI8, 4UFY, 4UFU, 4UI4.

4.2. Chemical synthesis

4.2.1. General materials and methods

Chemical reagents were purchased from Sigma, Aldrich, Fluka, Acros, Lancaster and Novabiochem. Dry THF was obtained by distillation over Na / benzophenone. All other solvents were purchased from Fisher Scientific. Analytical TLC was performed using silica gel 60 F254 pre-coated on Al sheets (0.25 mm thickness). Column chromatography was performed on silica gel 60 (35-70 mm). Melting points were recorded on a Reichert-Jung Kofler block apparatus and are uncorrected. ^{1}H and ^{13}C NMR spectra were recorded using Bruker Advance DPX 500 MHz and 400 MHz (^{1}H) instruments. High resolution mass spectra were determined using electrospray ionisation (ES) on a Bruker Daltonics MicroTOF instrument and were calibrated with Na^{+} HCO_2^{-}. The brine was saturated. Experiments were conducted at ambient temperature, unless otherwise stated. Solutions in organic solvents were dried with anhydrous $MgSO_4$. Solvents were evaporated under reduced pressure. Details are given below for one example of each reaction type; the syntheses and characterisation of analogues are reported in the Supplementary Information. The 8-methylquinazolinones **18** were synthesised as reported in our preliminary communication.[40]

4.2.2. 2-Phenylquinazolin-4-one (13a)

2-Aminobenzamide **12** (400 mg, 2.9 mmol) was heated with benzaldehyde (310 mg, 2.9 mmol) and $NaHSO_3$ (454 mg, 4.3 mmol) at 150°C for 3.5 h in N,N-dimethylacetamide (3.5 mL) in an open flask. The cooled mixture was poured into water and the precipitate was collected by filtration. Chromatography (CH_2Cl_2 → CH_2Cl_2 / MeOH 97:3) and recrystallisation (EtOAc) gave **13a** (350 mg, 54%) as white crystals: mp 235-236°C (lit. [58] mp 235-237°C); ^{1}H NMR ($(CD_3)_2SO$) δ 7.48-7.59 (4 H, m, Ph 2,4,6-H_3 + 6-H), 7.72 (1 H, d, *J* = 8.0 Hz, 8-H), 7.81 (1 H, t, *J* = 8.0 Hz, 7-H), 8.13-8.18 (3 H, m, Ph 3,5-H_2 + 5-H), 12.49 (1 H, s, NH); ^{13}C NMR ($(CD_3)_2SO$) (HSQC / HMBC) δ 120.97 (C-4a), 125.83 (5-C), 126.54 (6-C), 127.44 (Ph 3,5-C_2), 128.56 (Ph 2,6-C_2), 131.35 (Ph 4-C), 132.70 (Ph 1-C), 134.54 (7-C), 148.69 (8a-C), 152.27 (2-C), 162.17 (4-C).

4.2.3. 2-(4-Trifluoromethylphenyl)quinazolin-4-one (13c)

Compound **14c** (700 mg, 2.3 mmol) was stirred with aq. NaOH (0.5 M, 15 mL) at 60°C for 3.5 h. The mixture was acidified by addition of aq. HCl (9 M) to pH 2. The precipitate was collected by filtration and dried under vacuum to give **13c** (620 mg, 94%) as a white solid: mp 305-308°C (lit. [59] mp 306-308°C); ^{1}H NMR ($(CD_3)_2SO$) δ 7.56 (1 H, t, *J* = 7.5 Hz, 6-H), 7.78 (1 H, d, *J* = 7.5 Hz, 8-H), 7.87 (1 H, m, 7-H), 7.30 (2 H, d, *J* = 8.0, Ph 3,5-H_2), 8.18 (1 H, dd, *J* = 8.0, 1.0 Hz, 5-H), 8.37 (2 H, d, *J* = 8.0 Hz, Ph 2,6-H_2), 12.75 (1 H, s, NH); ^{13}C NMR ($(CD_3)_2SO$) (HSQC / HMBC) δ 121.21 (4a-C), 123.96 (q, *J* = 270.3 Hz, CF_3), 125.50 (q, *J* = 3.5 Hz, Ph

3,5-C_2), 125.12 (5-C), 127.12 (6-C), 127.69 (8-C), 128.73 (Ph 2,6-C_2), 130.98 (q, *J* = 32.1 Hz, Ph 4-C), 134.74 (7-C), 136.61 (Ph 1-C), 148.44 (8a-C), 151.17 (2-C), 162.10 (4-C).

4.2.4. 2-(4-Hydroxyphenyl)quinazolin-4-one (13j)

Compound **13i** (467 mg, 1.9 mmol) was boiled under reflux with BBr_3 in CH_2Cl_2 (1.0 M, 11 mL) for 3 h. The solvent was evaporated. The residue was stirred with aq. NaOH (2.5 M, 100 mL) for 3 h. The mixture was acidified by addition of aq. HCl (9 M) to pH 2. The mixture was extracted with ethyl acetate (3 × 20 mL). Drying and evaporation gave **13j** (420 mg, 95%) as a white solid: mp 258-261°C (lit. [60] mp 261-263°C); ^{1}H NMR ($(CD_3)_2SO$) δ 6.88 (2 H, d, *J* = 8.5 Hz, Ph 3,5-H_2), 7.46 (1 H, m, 6-H), 7.67 (1 H, d, *J* = 8.0 Hz, 8-H), 7.80 (1 H, m, 7-H), 8.08 (2 H, d, *J* = 8.5 Hz, Ph 2,6-H_2), 8.12 (1 H, dd, *J* = 8.0, 1.5 Hz, 5-H), 10.15 (1 H, s, OH), 12.30 (1 H, s, NH); ^{13}C NMR ($(CD_3)_2SO$) (HSQC / HMBC) δ 115.34 (Ph 3,5-C_2), 120.57 (4a-C), 123.19 (Ph 1-C), 125.79 (5-C), 125.91 (6-C), 127.18 (8-C), 129.56 (Ph 2,6-C_2), 134.50 (7-C), 149.04 (8a-C), 152.11 (2-C), 160.53 (Ph 4-C), 162.30 (4-C).

4.2.5. 2-Benzamidobenzamide (14a)

Dry pyridine (151 mg, 1.2 mmol) was added to **12** (200 mg, 1.47 mmol) in dry THF (4.0 mL), followed by benzoyl chloride (228 mg, 1.6 mmol) in dry THF (4.0 mL). The mixture was stirred under Ar for 16 h. Evaporation and chromatography (EtOAc / CH_2Cl_2 2:3) gave **14a** (351 mg, 99%) as a white solid: mp 233-235°C (lit. [61] mp 234°C); ^{1}H NMR ($(CD_3)_2SO$) δ 7.17-7.19 (1H, m, 5-H), 7.56-7.59 (3 H, m, 4-H + Ar 3,5-H_2), 7.63 (1 H, m, Ar 4-H), 7.65 (1 H, br, s, N*H*H), 7.89 (1 H, dd, *J* = 8.0, 1.5 Hz, 6-H), 7.94-7.96 (2 H, m, Ar 2,6-H_2), 8.43 (1 H, brs, NH*H*), 8.72 (1 H, dd, *J* = 8.5, 1.0 Hz, 3-H), 12.96 (1 H, s, NH); ^{13}C ($(CD_3)_2SO$) (HSQC / HMBC) δ 119.15 (1-C), 120.00 (3-C), 122.63 (5-C), 126.92 (Ar 2,6-C_2), 128.73 (6-C), 128.92 (Ar 3,5-C_2), 132.03 (Ar 4-C), 132.58 (4-C), 140.08 (2-C), 134.60 (Ar 1-C), 164.37 (NHCO), 171.15 ($CONH_2$).

4.2.6. 2-Amino-3-methoxybenzamide (16b)

Compound **15b** (3.00 g, 17.9 mmol) in dry DMF (80 mL) was treated with 1,1-carbonyldiimidazole (3.19 g, 19.7 mmol) at 70°C under Ar for 1 h, after which aq. NH_3 (35%, 50 mL) was added dropwise and the mixture was stirred for 16 h. The mixture was cooled to 20°C and was diluted with EtOAc (100 mL). The mixture was washed twice with water and twice with brine. Drying and evaporation gave **16b** (2.38 g, 80%) as a white solid: mp 139-141°C (lit. [40] mp 139-141°C); ^{1}H NMR ($(CD_3)_2SO$) δ 3.77 (3 H, s, Me), 6.23 (2 H, br, Ar-NH_2), 6.44 (1 H, t, *J* = 8.0 Hz, 5-H), 7.04 (1 H, dd, *J* = 7.6, 0.8 Hz, 6-H), 7.03 (1 H, brs, CONH*H*), 7.16 (1 H, dd, *J* = 8.0, 1.2 Hz, 4-H), 7.67 (1 H, brs, CON*H*H); ^{13}C NMR ($(CD_3)_2SO$) (HSQC / HMBC) δ 55.53 (Me), 111.98 (6-C), 113.38 (3-C), 113.64 (5-C), 120.42 (4-C), 140.19 (1-C), 146.88 (2-C), 171.19 (C=O).

4.2.7. 2-(4-Aminophenyl)-8-methoxyquinazolin-4-one (20h)

Compound **20g (**100 mg, 0.34 mmol) was stirred with Pd/C (10%, 100 mg) and $^+NH_4$ HCO_2^- (212 mg, 3.4 mmol) in MeOH (6 mL) and DMF (6 mL) under Ar for 3 h. The mixture was filtered (Celite). Evaporation and chromatography (EtOAc / petroleum ether 4:1) gave **20h** (65 mg, 83%) as a white solid: mp 271-274°C (lit. [47] mp 263-265°C); ^{1}H NMR ($(CD_3)_2SO$) δ 3.92 (3 H, s, Me), 5.80 (2 H, s, NH_2), 6.63 (2 H, dt, *J* = 8.5, 2.5 Hz, Ar 3,5-H_2), 7.29-7.34 (2 H, m, 6-H + 7-H), 7.64 (1 H, dd, *J* = 7.5, 2.0 Hz, 5-H), 7.95 (2 H, dt, *J* = 9.5, 2.5 Hz, Ar 2,6-

H_2), 12.09 (1 H, s, NH); ^{13}C NMR ($(CD_3)_2SO$) (HSQC / HMBC) δ 55.97 (OMe), 113.01 (Ar 3,5-C_2), 114.91 (7-C), 116.91 (5-C), 119.11 (Ar 1-C), 121.28 (4a-C), 125.38 (6-C), 129.07 (Ar 2,6-C_2), 140.05 (8a-C), 151.11 (Ar 4-C), 151.98 (2-C), 154.32 (8-C), 162.30 (4-C).

4.2.8. 2-Amino-4-methylbenzamide (25)

Compound **22** (3.00 g, 19.8 mmol) in dry DMF (100 mL) under Ar was treated with EDC.HCl (4.17 g, 21.8 mmol) and HOBt (3.33 g, 21.8 mmol) for 3 h, after which aq. NH_3 (35%, 20 mL) was added and the mixture was stirred for 16 h. The evaporation residue, in EtOAc, was washed twice with water and with brine. Drying and evaporation gave **25** (2.04 g, 69%) as an off-white solid: mp 151-153°C (lit. [62] mp 148°C); ^{1}H NMR ($(CD_3)_2SO$) δ 2.22 (3 H, s, Me), 6.35 (1 H, dd, *J* = 8.0, 1.2, 5-H), 6.52 (1 H, d, *J* = 0.5 Hz, 3-H), 6.57 (2 H, s, NH_2), 6.95 (1 H, brs, CON*H*H), 7.48 (1 H, d, *J* = 8.0 Hz, 6-H), 7.65 (1 H, brs, CONH*H*); ^{13}C NMR ($(CD_3)_2SO$) (HSQC / HMBC) δ 21.03 (Me), 111.14 (1-C), 115.61 (5-C), 116.44 (3-C), 128.77 (6-C), 141.55 (2-C), 150.31 (4-C), 171.19 (C=O).

4.2.9. 2-(4-(Phenylmethoxycarbonylaminomethyl)phenyl)benzamide (35)

Compound **34** (4.00 g, 26.5 mmol) in aq. K_2CO_3 (1.0 M, 144 mL) was stirred vigorously with BnOCOCl (4.52 g, 26.5 mmol) for 16 h. The precipitate was collected by filtration and dried. This material was stirred with $SOCl_2$ (10 mL) under Ar for 16 h. The evaporation residue was suspended in CH_2Cl_2 and filtered. Evaporation gave the crude acyl chloride, which was used immediately. This acyl chloride in dry THF (70 mL) was stirred with 2-aminobenzamide **12** (1.96 g, 14.4 mmol), pyridine (1.48 g, 18.7 mmol) and DMAP (0.35 g, 2.88 mmol) under Ar for 16 h. The evaporation residue, in EtOAc, was washed twice with water and twice with brine. Drying, evaporation and chromatography (EtOAc / CH_2Cl_2 2:3) gave **35** (5.1 g, 88%) as a white solid: mp 180-183°C; ^{1}H NMR ($(CD_3)_2SO$) δ 4.29 (2 H, d, *J* = 6.0 Hz, CH_2), 5.06 (2 H, s, OCH_2), 7.17-7.19 (1 H, m, 4-H), 7.30-7.38 (5 H, m, Cbz Ph 3,5-H_2 + Ph 2,6-H_2 + Ph 4-CH_2NH), 7.44 (2 H, d, *J* = 8.0 Hz, Cbz Ph 2,6-H_2), 7.57-7.59 (1 H, m, 5-H), 7.86-7.90 (4 H, m, Ph 2,6-H_2 + CON*H*H + H-3), 7.94 (1 H, t, *J* = 7.5 Hz, Cbz Ph 4-H), 8.44 (1 H, s, CONH*H*), 8.70 (1 H, d, *J* = 8.5 Hz, 6-H), 12.95 (1 H, s, 2-NH); ^{13}C NMR ($(CD_3)_2SO$) (HMBC / HSQC) δ 43.58 (CH_2NH), 65.55 (OCH_2), 119.08 (1-C), 120.02 (6-C), 122.64 (4-C), 127.08 (Ph 3,5-C_2), 127.42 (Cbz Ph 2,6-C_2), 127.85 (Ph 2,6-C_2), 127.89 (3-C), 128.42 (Cbz 3,5-C_2), 128.79 (Cbz Ph 4-C), 132.66 (5-C), 133.24 (Ph 1-C), 137.13 (Cbz Ph 1-C), 140.18 (2-C), 144.08 (Ph 4-C), 156.47 (Cbz NHCO), 164.26 (NHCO), 171.20 ($CONH_2$); MS (ES) *m/z* 426.1437 $[M + Na]^+$ ($C_{23}H_{21}N_3NaO_4$ requires 426.1430).

4.2.10. 2-(4-(Phenylmethoxycarbonylaminomethyl)phenyl)quinazolin-4-one (38)

Compound **35** (100 mg, 0.25 mmol) was stirred with aq. K_2CO_3 (1.0 M, 50 mL) at 100°C for 16 h. The cooled reaction mixture was acidified to pH~1. The precipitate was collected by filtration. Chromatography (EtOAc / petroleum ether 3:2) gave **38** (90 mg, 94%) as a white solid: mp 244-248°C; ^{1}H NMR ($(CD_3)_2SO$) δ 4.30 (2 H, d, *J* = 6.5 Hz, Ar 4-CCH_2), 5.07 (2 H, s, Cbz CH_2), 7.32-7.38 (5 H, m, Cbz Ph-H_5), 7.42 (2 H, d, *J* = 8.5 Hz, Ar 3,5-H_2), 7.52 (1 H, m, 6-H), 7.74 (1 H, d, *J* = 8.0 Hz, 8-H), 7.84 (1 H, m, 7-H), 7.94 (1 H, t, *J* = 6.0 Hz, CH_2NH), 8.13-8.16 (3H, m, Ar 2,6-H_2 + 5-H), 12.55 (NH); ^{13}C ($(CD_3)_2SO$) (HMBC / HSQC) δ 44.25 (Ar 4-C*C*H_2), 66.17 (Cbz CH_2), 121.62 (4a-C), 126.54 (5-C), 127.19 (6-C), 127.76 (Ar 3,5-C_2), 128.13 (8-C), 128.47 (Ar 2,6-C_2 + Cbz 2,6-C_2), 128.52 (Cbz 4-C), 129.06 (Cbz 3,5-H_2), 131.96 (Ar 1-C), 135.28 (7-C), 137.80 (Cbz 1-C), 144.05 (Ar 4-C), 149.52 (8a-C), 152.84 (2-

C), 157.13 (Cbz-CO), 163.10 (4-C); MS (ES) *m/z* 408.1317 $[M + Na]^+$ ($C_{23}H_{19}N_3NaO_3$ requires 408.1324].

4.2.11. 2-(4-(Aminomethylphenyl)quinazolin-4-one hydrobromide (41)

Compound **38** (0.15 g, 0.39 mmol) was stirred with HBr in AcOH (33%, 1.5 mL) for 16 h. Evaporation gave **41** (0.13 g, 92%) as a white solid: mp 277-285°C; ^{1}H NMR (CD_3OD) δ 4.34 (2 H, s, CH_2), 7.76 (1 H, m, 6-H), 7.85 (2 H, d, *J* = 8.0 Hz, Ar 3,5-H_2), 7.90 (1 H, d, *J* = 8.5 Hz, 8-H), 8.03 (1 H, m, 7-H), 8.14 (2 H, d, *J* = 8.0 Hz, Ar 2,6-H_2), 8.36 (1 H, dd, *J* = 8.0, 1.0 Hz, 5-H); ^{13}C NMR (CD_3OD) (HMBC / HSQC) δ 43.72 (CH_2), 121.30 (4a-C), 122.36 (8-C), 128.32 (5-C), 129.28 (Ar 1-C), 130.23 (6-C), 130.83 (Ar 2,6-C_2), 131.00 (Ar 3,5-C_2), 137.54 (7-C), 140.85 (Ar 4-C), 141.58 (8a-C), 158.58 (2-C), 161.40 (4-C); HRMS (ES) *m/z* 252.1140 $[M + H]^+$ ($C_{15}H_{14}N_3O$ requires 252.1137].

4.2.12. 2-Phenylthieno[3,4-d]pyrimidin-4-one (45)

Compound **44** (580 mg, 2.8 mmol) was stirred with K_2CO_3 (1.17 g, 8.5 mmol), CuBr (40 mg, 0.28 mmol) and $BnNH_2$ (610 mg, 5.7 mmol) at 125°C in an open flask for 16 h in DMSO (28 mL). The mixture was diluted with EtOAc (30 mL) and was washed twice with water and twice with brine. Drying, evaporation, chromatography (CH_2Cl_2 → EtOAc / CH_2Cl_2 1:5) and recrystallisation (CH_2Cl_2) gave **45** (102 mg, 16%) as a yellow solid: mp 280-283°C (lit. [46] 275-277°C); ^{1}H NMR ((CD_3)$_2$SO) δ 7.50-7.56 (3 H, m, Ar 3,4,5-H_3), 7.86 (1 H, d, *J* = 3.5 Hz, 7-H), 8.10 (2 H, m, Ph 2,6-H_2), 8.51 (1 H, d, *J* = 3.5 Hz, 5-H), 11.93 (1 H, s, NH); ^{13}C NMR ((CD_3)$_2$SO) (HSQC / HMBC) δ 118.32 (7-C), 125.01 (4a-C), 127.61 (Ph 2,6-C_2), 127.89 (5-C), 128.50 (Ph 3,5-C_2), 131.04 (Ph 4-C), 132.91 (Ph 1-C), 148.72 (7a-C), 150.86 (2-C), 158.91 (4-C).

4.3. Enzyme assays

Test compounds were assayed for inhibition of tankyrase-1, tankyrase-2, PARP-1 and PARP-2 activity as described previously [31, 33, 40].

4.4. Mouse embryonic stem cell culture and Wnt signalling reporter assay

The cell lines used in this study were E14Tg2A (a mouse embryonic stem cell (mESC) line) and TLg2 (derived from E14Tg2A and harboring a Wnt-responsive element driving eGFP) [51,54]. The activity of the test compounds was assessed as described previously [51]. Briefly, TLg2 cells were plated on gelatin at low density (4×10^4 cells per well in a 6-well plate) in either serum + LIF (standard culture conditions) or in the presence of N2B27 (differentiating conditions) in the absence (untreated) or presence (treated) of test compound (10 μM). The medium was refreshed daily and the Wnt activity was assessed by flow cytometry using a LSR Fortessa cytometer (BD Bioscience). Live single cells were selected on forward and side scatter area, side scatter width *vs.* area and DAPI exclusion (405 laser and 450/50 filter set). Expression of eGFP was assessed using the 488 laser and 530/30 filter set. Data were analyzed and presented using Flowjo software (TreeStar). No test compound was toxic during the 3 d of treatment.

Acknowledgements

The authors thank Worldwide Cancer Research for generous financial support (grant No. 10-0104). Protein crystallographic work was funded by Biocenter Oulu and Academy of Finland

(grant No. 266922). The use of the facilities and expertise of the Biocenter Oulu core facility, a member of Biocenter Finland and Instrut-FI, is gratefully acknowledged. Protein crystallographic experiments were performed on the ID23-2 beamline at the European Synchrotron Radiation Facility (ESRF), Grenoble, France and the Diamond Light Source (Didcot, UK) Beamlines I04-1 and I03. We are grateful to Local Contracts at ESRF and the Diamond Light Source for providing assistance in using beamlines. The research leading to these results has received funding from the European Community's Seventh Framework Programme (FP7/2007-2013) under BioStruct-X (grant agreement No283570).

Supplementary data

Supplementary data associated with this article can be found in the online version at ##################.

References

[1] D. V. Ferraris, Evolution of poly(ADP-ribose) polymerase-1 (PARP-1) inhibitors. From concept to clinic, J. Med. Chem. 53 (2010) 4561-4584.

[2] S. Smith, I. Giriat, A. Schmitt, T. de Lange, Tankyrase, a poly(ADP-ribose) polymerase at human telomeres, Science 282 (1998) 1484-1487.

[3] R. J. Lyons, R. Deane, D. K. Lynch, Z.-S. J. Ye, G. M. Sanderson, H. J. Eyre, G. R. Sutherland, R. J. Daly, Identification of a novel human tankyrase through its interaction with the adaptor protein Grb14, J. Biol. Chem. 276 (2001) 17172-17180.

[4] S. Gelmini, M. Poggesi, V. Distante, S. Bianchi, L. Simi, M. Luconi, C. Casini Raggi, L. Cataliotti, M. Pazzaglia, C. Orlando, Tankyrase, a positive regulator of telomere elongation, is over expressed in human breast cancer, Cancer Lett. 216 (2004) 81-87.

[5] S. Zimmermann, U. M. Martens, Telomeres and telomerase as targets for cancer therapy, Cell. Mol. Life Sci. 64 (2007) 906-921.

[6] M. Seimiya, The telomeric PARP, tankyrases, as targets for cancer therapy, Br. J. Cancer, 94 (2006) 341-345.

[7] P. Chang, M. Coughlin, T. J. Mitchison, Tankyrase-1 polymerization of poly(ADP-ribose) is required for spindle structure and function, Nature Cell Biol. 7 (2005) 1133-1139.

[8] J. N. Dynek, S. Smith, Resolution of sister telomere association is required for progression through mitosis, Science 304 (2004) 97-100.

[9] W. Chang, J. N. Dynek, S. Smith, NuMA is a major acceptor of poly(ADP-ribosyl)ation by tankyrase 1 in mitosis, Biochem. J. 391 (2005) 177-184.

[10] T.-Y. J. Yeh, J. I. Sbodio, Z.-Y. Tsun, B. Luo, N.-W. Chi, Insulin-stimulated exocytosis of GLUT4 is enhanced by IRAP and its partner tankyrase, Biochem. J. 402 (2007) 279-290.

[11] H.-L. Guo, C. Zhang, Q. Liu, Q. X. Li, G. Lian, D. Wu, X. Li, W. Zhang, Y. Shen, Z. Ye, S.-Y. Lin, S.-C. Lin, The Axin/TNKS complex interacts with KIF3A and is required for insulin-stimulated GLUT4 translocation, Cell Res. 22 (2012) 1246-1257.

[12] Z. Deng, C. Atanasiu, K. Zhao, R. Marmorstein, J. I. Sbodio, N.-W. Chi, P. M. Leiberman, Inhibition of Epstein-Barr virus OriP function by tankyrase, a telomere-associated poly-ADP ribose polymerase that binds and modifies EBNA1, J. Virol. 79 (2005) 4640-4650.

[13] Z. Li, Y. Yamauchi, M. Kamakura, T. Murayama, F. Goshima, H. Kimura, Y. Nishiyama, Herpes simplex virus requires poly(ADP-ribose) polymerase activity for efficient replication and induces extracellular signal-related kinase-dependent phosphorylation and ICP0-dependent nuclear localization of tankyrase 1, J. Virol. 86 (2012) 492-503.

[14] S.-M. A. Huang, Y. M. Mishina, S. Liu, A. Cheung, F. Stegmeier, G. A. Michaud, O. Charlat, E. Wiellette, Y. Zhang, S. Wiessner, M. Hild, X. Shi, C. J. Wilson, C. Mickanin, V. Myer, A. Fazal, R. Tomlinson, F. Serluca, W. Shao, H. Cheng, M. Shultz, C. Rau, M. Schirle, J. Schlegl, S. Ghidelli, S. Fawell, C. Lu, D. Curtis, M. W. Kirschner, C. Lengauer, P. M. Finan, J. A. Tallarico, T. Bouwmeester, J. A. Porter, A. Bauer, F. Cong, Tankyrase inhibition stabilizes axin and antagonizes Wnt signalling, Nature 461 (2009) 614-620.

[15] B. D. White, A. J. Chien, D. W. Dawson, Dysregulation of Wnt/β-catenin signaling in gastrointestinal cancers, Gastroenterology 142 (2012) 219-232.

[16] M. Katoh, H. Kirikoshi, H. Terasaki, K. Shiokawa, WNT2B2 mRNA, up-regulated in primary gastric cancer, is a positive regulator of the WNT–β-catenin–TCF signaling pathway, Biochem. Biophys. Res. Commun. 289 (2001) 1093-1098.

[17] Y. Miyoshi, K. Iwao, Y. Nagasawa, T. Aihara, Y. Sasaki, S. Imaoka, M. Murata, T. Shimano, Y. Nakamura, Activation of the β-catenin gene in primary hepatocellular carcinomas by somatic alterations involving exon 3, Cancer Res. 58 (1998) 2524-2527.

[18] M. Katoh, Expression and regulation of WNT1 in human cancer: Up-regulation of WNT1 by β-estradiol in MCF-7 cells, Int. J. Oncol. 22 (2003) 209-212.

[19] R. Najdi, R. F. Holcombe, M. L. Waterman, Wnt signaling and colon carcinogenesis: Beyond APC, J. Carcinog. 10 (2011) 5.

[20] J. Waaler, O. Machon, L. Tumova, H. Dinh, V. Korinek, S. R. Wilson, J. E. Paulsen, N. M. Pedersen, T. J. Eide, O. Machonova, D. Gradl, A. Voronkov, J. P. von Kries, S. Krauss, A novel tankyrase inhibitor decreases canonical Wnt signaling in colon carcinoma cells and reduces tumor growth in conditional APC mutant mice, Cancer Res. 72 (2012) 2822-2832.

[21] J. Waaler, O. Machon, J. P. von Kries, S. R. Wilson, E. Lundenes, D. Wedlich, D. Gradl, J. E. Paulsen, O. Machonova, J. L. Dembinski, H. Dinh, S. Krauss, Novel synthetic antagonists of canonical Wnt signaling inhibit colorectal cancer cell growth, Cancer Res. 71 (2011) 197-205.

[22] N. Sidorova, L. Zavalishina, S. Kurchashova, N. Korsakova, V. Nazhimov, G. Frank, A. Kuimov, Immunohistochemical detection of tankyrase 2 in human breast tumors and normal renal tissue, Cell Tissue Res. 323 (2006) 137-145.

[23] S. Gelmini, M. Poggesi, P. Pinzani, S. C. Mannurita, F. Cianci, R. Valanzano, C. Orlando, Distribution of Tankyrase-1 mRNA expression in colon cancer and its prospective correlation with progression stage, Oncol. Rep. 16 (2006) 1261-1266.

[24] Y. V. Shebzukhov, I. N. Lavrik, J. Karbach, S. V. Khlgatian, E. P. Koroleva, P. V. Belousov, K. N. Kashkin, A. Knuth, E. Jager, N.-W. Chi, D. V. Kuprash, S. A. Nedospasov, Human tankyrases are aberrantly expressed in colon tumors and contain multiple epitopes that induce humoral and cellular immune responses in cancer patients, Cancer Immunol. Immunother. 57 (2008) 871-881.

[25] L. J. Campbell, C. Fidler, H. Eagleton, A. Peniket, R. Kusec, S. Gal, T. J. Littlewood, J. S. Wainscoat, J. Boultwood, *hTERT*, the catalytic component of telomerase, is downregulated in the haematopoietic stem cells of patients with chronic myeloid leukaemia, Leukemia 20 (2006) 671-679.

[26] A. Shervington, R. Patel, C. Lu, N. Cruickshanks, R.; Lea, G. Roberts, T. Dawson, L. Shervington, Telomerase subunits expression variation between biopsy samples and cell lines derived from malignant glioma, Brain Res. 1134 (2007) 45-52.

[27] B. Tang, J. Wang, J. Fang, B. Jiang, M. Zhang, Y. Wang, Z Yang, Expression of TNKS1 is correlated with pathologic grade and Wnt/β-catenin pathway in human astrocytomas, J. Clin. Neurosci. 19 (2012) 139-143.

[28] J. Gao, J. Zhang, Y. Long, Y. Tian, X. Lu, Expression of tankyrase 1 in gastric cancer and its correlation with telomerase activity, Pathol. Oncol. Res. 17 (2011) 685-690.

[29] S. Gelmini, S. Quattrone, F. Malentacchi, D. Villari, F. Travaglini, G. Giannarini, A. Della Melina, M. Pazzagli, G. Nicita, C. Selli, C. Orlando, Tankyrase-1 mRNA expression in bladder cancer and paired urine sediment: preliminary experience, Clin. Chem. Lab. Med. 45 (2007) 862-866.

[30] M. Narwal, T. Haikarainen, A. Fallarero, P. M. Vuorela, L. Lehtiö, Screening and structural analysis of flavones inhibiting tankyrases, J. Med. Chem. 56 (2013) 3507-3517.

[31] H. A. Paine, A. Nathubhai, E. C. Y. Woon, P. T. Sunderland, P. J. Wood, M. F. Mahon, M. D. Lloyd, A. S. Thompson, T. Haikarainen, M. Narwal, L. Lehtiö, M. D. Threadgill, Exploration of the nicotinamide-binding site of the tankyrases, identifying 3-arylisoquinolin-1-ones as potent and selective inhibitors in vitro, Bioorg. Med. Chem. 23 (2015) 5891-5908.

[32] K. Kumpan, A. Nathubhai, C. Zhang, P. J. Wood, M. F. Mahon, M. D. Lloyd, A. S. Thompson, T. Haikarainen, L. Lehtiö, M. D. Threadgill, Structure-based design, synthesis and evaluation in vitro of arylnaphthyridinones, arylpyridopyrimidinones and their tetrahydro derivatives as inhibitors of the tankyrases, Bioorg. Med. Chem. 23 (2015) 3013-3032.

[33] T. Haikarainen, J. Koivunen, M. Narwal, H. Venkannagari, E. Obaji, P. Joensuu, T. Pihlajaniemi, L. Lehtiö, *para*-Substituted 2-phenyl-3,4-dihydroquinazolin-4-ones as potent and selective tankyrase inhibitors, ChemMedChem. 8 (2013) 1978-1985.

[34] M. Narwal, H. Venkannagari, L. Lehtiö, Structural basis of selective inhibition of human tankyrases, J. Med. Chem. 55 (2012) 1360-1367.

[35] H. Gunaydin, Y. Gu, X. Huang, Novel binding mode of a potent and selective tankyrase inhibitor, PLOS One 7 (2012) e33740.

[36] H. Bregman, N. Chakka, A. Guzman-Perez, A.; H. Gunaydin, Y. Gu, X. Huang, V. Berry, J. Liu, Y. Teffera, L. Huang, B. Egge, E. L. Mullady, S. Schneider, P. S. Andrews, A. Mishra, J. Newcomb, R. Serafino, C. A. Strathdee, S. M. Turci, C. Wilson, E. F. DiMauro, Discovery of novel, induced-pocket binding oxazolidinones as potent, selective, and orally bioavailable tankyrase inhibitors, J. Med. Chem. 56 (2013) 4320-4342.

[37] T. Karlberg, N. Markova, I. Johansson, M. Hammarström, P. Schütz, J. Weigelt, H. Schüler, Structural basis for the interaction between tankyrase-2 and a potent Wnt-signaling inhibitor, J. Med. Chem. 53 (2010) 5352-5355.

[38] T. Haikarainen, H. Venkannagari, M. Narwal, E. Obaji, H.-W. Lee, Y. Nkizinkiko, L. Lehtiö, Structural basis and selectivity of tankyrase inhibition by a Wnt signaling inhibitor WIKI4, PLOS One 8 (2013) e65404.

[39] L. Lehtiö, R. Collins, S. van den Berg, A. Johansson, L.-G. Dahlgren, M. Hammarström, T. Helleday, L. Holmberg-Schiavone, T. Karlberg, J. Weigelt, Zinc binding catalytic domain of human tankyrase 1, J. Mol. Biol. 379 (2008) 136-145.

[40] A. Nathubhai, P. J. Wood, M. D. Lloyd, A. S. Thompson, M. D. Threadgill, Design and discovery of 2-arylquinazolin-4-ones as potent and selective inhibitors of tankyrases, ACS Med. Chem. Lett. 4 (2013) 1173-1177.

[41] Z. Hua, H. Bregman, J. L. Buchanan, N. Chakka, A. Guzman-Perez, H. Gunaydin, X. Huang, Y. Gu, V. Berry, J. Liu, Y. Teffera, L. Huang, B. Egge, R. Emkey, E. L. Mullady, S. Schneider, P. S. Andrews, L. Acquaviva, J. Dovey, A. Mishra, J. Newcomb, D. Saffran, R. Serafino, C. A. Strathdee, S. M. Turci, M. Stanton, C. Wilson, E. F. DiMauro, Development of novel dual binders as potent, selective, and orally bioavailable tankyrase inhibitors, J. Med. Chem. 56 (2013) 10003-10015.

[42] M. D. Shultz, A. K. Cheung, C. A. Kirby, B. Firestone, J. Fan, C. H.-T. Chen, Z. Chen, D. N. Chin, L. DiPietro, A. Fazal, Y. Feng, P. D. Fortin, T. Gould, B. Lagu, H. Lei, F. Lenoir, D. Majumdar, E. Ochala, M. G. Palermo, L. Pham, M. Pu, T. Smith, T. Stams, R. C. Tomlinson, B. B. Touré, M. Visser, R. M. Wang, N. J. Waters, W. Shao, Identification of NVP-TNKS656: The use of structure-efficiency relationships to generate a highly potent, selective, and orally active tankyrase inhibitor, J. Med. Chem. 56 (2013) 6495-6511.

[43] M. Tišler, B. Stanovnik, Z. Zrimšek, C. Stropnik, C. Heterocycles; CCI. A novel synthesis of heterocyclic thioformylamines, Synthesis (1981) 299-300.

[44] A. Nathubhai, R. Patterson, T. J. Woodman, H. E. C. Sharp, M. T. Y. Chui, H. H. K. Chung, S. W. S. Lau, J. Zheng, M. D. Lloyd, A. S. Thompson, M. D. Threadgill, N^3-Alkylation during formation of quinazolin-4-ones from condensation of anthranilamides and orthoamides, Org. Biomol. Chem. 9 (2011) 6089-6099.

[45] C. Schotten, Uber die Oxydation des Piperidins, Ber. deuts. Chem. Ges. 17 (1884) 2544-2547.

[46] A. E. Shinkwin, W. J. D. Whish, M. D. Threadgill, Synthesis of thiophenecarboxamides, thieno[3,4-*c*]pyridin-4(5*H*)-ones and thieno[3,4-*d*]pyrimidin-4(3*H*)-ones and preliminary evaluation as inhibitors of poly(ADP-ribose)polymerase (PARP), Bioorg. Med. Chem. 7 (1999) 297-308.

[47] R. J. Griffin, S. Srinivasan, K. Bowman, A. H. Calvert, N. J. Curtin, D. R. Newell, L. C. Pemberton, B. T. Golding, Resistance-modifying agents. 5. Synthesis and biological properties of quinazolinone inhibitors of the DNA repair enzyme poly(ADP-ribose) polymerase (PARP), J. Med. Chem. 41 (1998) 5247-5256.

[48] R. Pellicciari, E. Camaioni, G. Costantino, I. Formentini, P. Sabbatini, F. Venturoni, G. Eren, D. Bellocchi, A. Chiarugi, F. Moroni, On the way to selective PARP-2 inhibitors. Design, synthesis, and preliminary evaluation of a series of isoquinolinone derivatives, ChemMedChem 3 (2008) 914-923.

[49] P. T. Sunderland, E. C. Y. Woon, A. Dhami, A. Bergin, M. F. Mahon, P. J. Wood, L. A. Jones, S. R. Tully, M. D. Lloyd, A. S. Thompson, H. Javaid, N. M. B. Martin, M. D. Threadgill, 5-Benzamidoisoquinolin-1-ones and 5-(ω-carboxyalkyl)isoquinolin-1-ones as isoform-selective inhibitors of poly(ADP-ribose) polymerase 2 (PARP-2), J. Med. Chem. 2011, 54, 2049-2059.

[50] P. T. Sunderland, A. Dhami, M. F. Mahon, L. A. Jones, S. R. Tully, M. D. Lloyd, A. S. Thompson, H. Javaid, N. M. B. Martin, M. D. Threadgill, Synthesis of 4-alkyl-, 4-aryl- and 4-arylamino-5-aminoisoquinolin-1-ones and identification of a new PARP-2 selective inhibitor, Org. Biomol. Chem. 9 (2011) 881-891.

[51] F. Faunes, P. Hayward, S. Muñoz-Descalzo, S. S. Chatterjee, T. Balayo, J. Trott, A. Christoforou, A. Ferrer-Vaquer, A.-K. Hadjantonakis, R. Dasgupta, A. M. Arias, A membrane-associated β-catenin/Oct4 complex correlates with ground-state pluripotency in mouse embryonic stem cells, Development 140 (2013) 1171-1183.

[52] A. Ferrer-Vaquer, A. Piliszek, G. Tian, R. J. Aho, D. Dufort, A.-K. Hadjantonakis, A sensitive and bright single-cell resolution live imaging reporter of Wnt/β-catenin signaling in the mouse, BMC Developmental Biol. 10 (2010) 121-129.

[53] J. Wray, T. Kalkan, S. Gomez-Lopez, D. Eckardt, A. Cook, R. Kemler, A. Smith, Inhibition of glycogen synthase kinase-3 alleviates Tcf3 repression of the pluripotency network and increases embryonic stem cell resistance to differentiation, Nature Cell Biol. 13 (2011) 838-845.

[54] N. Lyashenko, M. Winter, D. Migliorini, R. Biechele, R. T. Moon, C. Hartmann, Differential requirement for the dual functions of β-catenin in embryonic stem cell self-renewal and germ layer formation, Nature Cell Biol. 13 (2011) 753-761.

[55] W. Kabsch, Automatic processing of rotation diffraction data from crystals of initially unknown symmetry and cell constants, J. Appl. Crystallogr. 26 (1993) 795-800.

[56] G. N. Murshudov, A. A. Vagin, E. J. Dodson, Refinement of macromolecular structures by the maximum-likelihood method, Acta Crystallogr. D Biol. Crystallogr. D53 (1997) 240-255.

[57] P. Emsley, K. Cowtan, Coot: model-building tools for molecular graphics, Acta Crystallogr. D Biol. Crystallogr. D60 (2004) 2126-2132.

[58] D. Zhao, Q. Shen, Y.-R. Zhou, J.-X. Li, KOtBu-mediated stereoselective addition of quinazolines to alkynes under mild conditions, Org. Biomol. Chem. 2013, 11, 5908-5912.

[59] A. Couture, H. Cornet, P. Grandclaudon, An expeditious synthesis of 2-aryl- and 2-alkylquinazolin-4(3*H*)-ones, *Synthesis* (1991) 1009-1010.

[60] R. Mekala, R. Akula, R. R. Kamaraju, C. K. Bannoth, S. Regati, J. Sarva, An efficient synthesis of 2-substituted quinazolin-4(3*H*)-ones catalyzed by iron(III) chloride, Synlett (2014) 821-826.

[61] P. Mani Chandrika, T. Yakaiah, A. Raghu Ram Rao, B. Narsaiah; N. Chakra Reddy, V. Sridhar, J. Venkateshwara Rao, Synthesis of novel 4,6-disubstituted quinazoline derivatives, their anti-inflammatory and anti-cancer activity (cytotoxic) against U937 leukemia cell lines, Eur. J. Med. Chem. 43 (2008) 846-852.

[62] H. Zhao, H. Hua; R. Qiao, Copper-catalyzed direct amination of *ortho*-functionalized haloarenes with sodium azide as the amino source, J. Org. Chem. 75 (2010) 3311-3316.

List of captions

List of Figures:

Figure 1. Structures of **1-11**, reported inhibitors of tankyrases.

Figure 2. Conformations of aroylanthranilamides **48** and 2-arylquinazolinones **49** in solution.

Figure 3. Crystal structures of Panel A **13b**, Panel B **13c**, Panel C **20b**, Panel D **20c**, Panel E **21b**, Panel F **21c**, Panel G **18b**, Panel H **18c**, Panel I **38** bound to TNKS-2. Overlay of **38** onto PARP-1 (panel J). Key residues are in purple and key H-bond interactions are shown as dashed lines.

Figure 4. Flow-cytometric analysis of TLg2 cells (and E14Tg2A control cells) grown under the indicated culture conditions. The black line indicates the median GFP fluorescence intensity of TLg2 cells cultured for 3 d in the presence of N2B27 medium and % is the percentage of cells found with fluorescence above that level under the various conditions.

List of Schemes:

Scheme 1. Synthesis of 2-arylquinazolin-4-ones **13a-j** and acylated anthranilamides **14a-i**. *Reagents and conditions*: i, ArCHO, $NaHCO_3$, $AcNMe_2$, 150°C, open flask; ii, $^+NH_4HCO_2^-$, Pd/C, MeOH, DMF; iii, BBr_3, CH_2Cl_2, reflux, then NaOH; iv, ArCOCl, pyridine, dry THF.

Scheme 2. Synthesis of 2-arylquinazolin-4-ones **18,20,21** with various 4'- and 8-substituents. *Reagents and conditions*: i, CDI or EDC, aq. NH_3, DMF; ii, ArCOCl, pyridine, dry THF; iii, aq. NaOH (0.5 M), 60 °C; iv, $^+NH_4HCO_2^-$, Pd/C, MeOH, DMF; v, BBr_3, CH_2Cl_2, reflux, then NaOH.

Scheme 3. Synthesis of 6- and 7-substituted 2-arylquinazolin-4-ones **31-33**. *Reagents and conditions*: i, CDI, aq. NH_3; ii, ArCOCl, pyridine, dry THF; iii, aq. NaOH (0.5 M).

Scheme 4. Synthesis of 2-arylquinazolin-4-ones **38-43** with extensions at the 4'-position. *Reagents and conditions*: i, CbzCl, aq. K_2CO_3; ii, $SOCl_2$, iii, **12** or **16a** or **27,** pyridine, dry THF; iv, aq. K_2CO_3 (1.0 M), 100°C; v, HBr, AcOH.

Scheme 5. Synthesis of thienopyrimidinone **45** and ferrocenylquinazolin-4-one **47**. *Reagents and conditions*: i, K_2CO_3, CuBr, $BnNH_2$, 125°C, DMSO, open flask; ii, ferrocenecarbonyl chloride, pyridine, dry THF; iii, aq. NaOH (0.5 M), 100°C.

List of Tables:

Table 1. Inhibition of TNKS-1, TNKS-2, PARP-1 and PARP-2 by 8-H 2-arylquinazolin-4-ones **13**. IC_{50} values in nM.

Table 2. Inhibition of TNKS-1, TNKS-2, PARP-1 and PARP-2 by 8-OMe 2-arylquinazolin-4-ones **20**. IC_{50} values in nM.

Table 3. Inhibition of TNKS-1, TNKS-2, PARP-1 and PARP-2 by 8-OH 2-arylquinazolin-4-ones **21**. IC_{50} values in nM.

Table 4. Inhibition of TNKS-1, TNKS-2, PARP-1 and PARP-2 by 8-OH 2-arylquinazolin-4-ones **18**. IC_{50} values in nM.

Table 5. Summary of the results obtained after flow cytometry analysis in TLg2 cells cultured in the indicated culture conditions. E14Tg2A cells are a non-fluorescent control cell line.